Title

Histone Demethylation and MYC Activation Enhance Translational Capacity in Response to Amino Acid Restriction

Author

Cheng, Chen

Publication Date

2017

Peer reviewed|Thesis/dissertation

UNIVERSITY OF CALIFORNIA

Los Angeles

Histone Demethylation and MYC Activation Enhance Translational Capacity in Response to Amino Acid Restriction

A dissertation submitted in partial satisfaction of the

requirements for the degree of Doctor of Philosophy

in Biological Chemistry

by

Chen Cheng

2017

ABSTRACT OF THE DISSERTATION

Histone Demethylation and MYC Activation Enhance Translational Capacity in Response to Amino Acid Restriction

by

Chen Cheng

Doctor of Philosophy in Biological Chemistry

University of California, Los Angeles, 2017

Professor Siavash K. Kurdistani, Chair

Nutrient limitation may elicit adaptive epigenetic changes but the nature and mechanisms of the cellular response to specific nutrient deficiencies are incompletely understood. We report that depriving human cells of amino acids (AAs) induces specific loss of histone H4 lysine 20 monomethylation (H4K20me1) from gene bodies and elevated binding of MYC at promoters genome-wide. These effects are most pronounced at ribosomal protein and translation initiation genes, which are transcriptionally upregulated, leading to enhanced protein synthetic capacity. Combination of SETD8, the H4K20 methyltransferase, depletion and MYC over-expression in rich media is required and sufficient to recapitulate the effects of AA restriction transcriptionally and functionally. Our data reveal an unexpected and epigenetically implemented increase in translational capacity when AAs are limiting. This adaptive response likely safeguards the proteome by making effective use of limited resources, and prepares the cell for swift initiation of protein synthesis when AAs are replenished.

The dissertation of Chen Cheng is approved.

Heather Christofk

John Colicelli

Kathrin Plath

Thomas Vondriska

Siavash K. Kurdistani, Committee Chair

University of California, Los Angeles

2017

TABLE OF CONTENTS

LIST OF FIGURES

LIST OF TABLE

ACKNOWLEDGMENTS

Manuscript contributors (a reproduction of this dissertation)

Histone Methylation Loss and MYC Activation Enhance Translational Capacity in Response to Amino Acid Restriction

Chen Cheng[1], Trent Su[1], Marco Morselli[2], and Siavash K. Kurdistani[1,3,4]*

[1]Department of Biological Chemistry, David Geffen School of Medicine, University of California, Los Angeles, California 90095, USA.
[2]Department of Molecular, Cell and Developmental Biology, University of California, Los Angeles, California 90095, USA.
[3]Department of Pathology and Laboratory Medicine, David Geffen School of Medicine, University of California, Los Angeles, California 90095, USA.
[4]Eli and Edythe Broad Center of Regenerative Medicine and Stem Cell Research, David Geffen School of Medicine, University of California, Los Angeles, California 90095, USA.

*Correspondence to: Siavash Kurdistani
310.794.5194
skurdistani@mednet.ucla.edu

I would like to thank both Trent Su and Marco Morselli for their contributions to this research. Marco generated the data for chromatin immunoprecipitation of H3K36me3 that was necessary for producing Figures 7A-7B. Trent not only provided several scripts to analyze the high-throughput sequencing data, but he also taught me a lot about sequencing data analysis.

VITA

Education:

In progress Ph.D. in Biological Chemistry

2006 M.S. in Biochemistry, University of Maine

2004 B.S. in Molecular and Cellular Biology and in Biochemistry, University of Maine

Research Positions:

2011- Graduate Student Researcher, UCLA, Department of Biological Chemistry, Laboratory of Siavash K. Kurdistani, MD

2006-2010 Staff Research Associate II, UCLA, Department of Molecular, Cell, and Developmental Biology, Laboratory of Robert B. Goldberg, PhD

2004-2006 Graduate Student Researcher, Department of Biological Sciences, University of Maine, Laboratory of Benildo G. de los Reyes, PhD

2003-2004 Student Researcher, Department of Biochemistry, Microbiology, and Molecular Biology, University of Maine, Laboratory of Mary E. Rumpho, PhD

2003-2004 Student Researcher, Department of Civil and Environmental Engineering, University of Maine, Laboratory of Jean D. MacRae, PhD

Publications:

1. Huang, C., Su, T., Xue, Y., **Cheng, C.**, Lay, F.D., McKee, R.A., Li, M., Vashisht, A., Wohlschlegel, J., Novitch, B.G., Plath, K., Kurdistani, S.K., Carey, M., 2017. Cbx3 maintains lineage specificity during neural differentiation. Genes & Development 31:241–246.

2. Le, B.H. †, **Cheng, C.** †, Bui, A.Q. †, Wagmaister, J.A., Henry, K.F., Pelletier, J., Kwong, L., Belmonte, M., Kirkbride, R., Horvath, S., Drews, G.N., Fischer, R.L., Okamuro, J.K., Harada, J.J., Goldberg, R.B., 2010. Global analysis of gene activity during Arabidopsis seed development and identification of seed-specific transcription factors. PNAS 107, 8063-8070.

3. **Cheng, C.** †, Yun, K.Y. †, Ressom, H.W., Mohanty, B., Bajic, V.B., Jia, Y., Yun, S.J., de los Reyes, B.G., 2007. An early response regulatory cluster induced by low temperature and hydrogen peroxide in seedlings of chilling-tolerant japonica rice. BMC genomics 8, 175.

4. Ballou, S.M., Yun, K.Y., **Cheng, C.**, de los Reyes, B.G., 2007. Cold sensitivity gradient in tuber-bearing Solanum based on physiological and transcript profiles. Crop Sci. 47, 2027–2035.

†Equal contributors

Teaching Positions during Ph.D. study at UCLA:

1. Spring 2015, TA, MCD BIO 104AL: Research Immersion Laboratory in Developmental Biology

2. Winter 2015, TA, MCD BIO 104AL: Research Immersion Laboratory in Developmental Biology

3. Spring 2014, TA, LIFESCI 3: Introduction to Molecular Biology

4. Fall 2013 and Winter 2014, TA, Medical School Human Biochemistry and Nutrition Lab

5. Winter 2013, TA, LIFESCI 23L: Introduction to Laboratory and Scientific Methodology

6. Spring 2012, TA, LIFESCI 4: Genetics

Research Presentations during Ph.D. study at UCLA:

1. Poster presentation, Title: Linking Translational Capacity to Gene Expression through Histone Methylation, Gordon Research Conference on Epigenetics, August 2016

2. Oral presentation, Title: Linking Translational Capacity to Gene Expression through Histone Methylation, UCLA Department of Biological Chemistry Monday Seminar Series, January 2016

3. Poster presentation, Title: Histone Methylation as a Metabolic Sensor for Gene Regulation, UCLA Department of Biological Chemistry Retreat, May 2013

4. Oral presentation, Title: Histone Methylation as a Metabolic Sensor for Gene Regulation, UCLA Department of Biological Chemistry Monday Seminar Series, April 2013

Funding during Ph.D. study at UCLA:

2010-2011 University Fellowship, UCLA Graduate Division

2015-2016 Dissertation Year Fellowship, UCLA Graduate Division

CHAPTER 1

Introduction

1.1 Chromatin modifications

All cells of a eukaryotic organism are encoded with the same genetic information, yet different cells, tissues, and organs show diverse and specialized functions mainly due to different gene expression programs. Therefore, gene expression patterns in different cell types need to be regulated appropriately. The chromatin state—the package of DNA with histone proteins—contributes to the control of diverse and specialized gene expression patterns. The regulation of chromatin state is influenced in part by the post-translational modifications (PTMs) on histones. As many as fifteen types of histone PTMs have been observed that include acetylation, methylation, phosphorylation, ubiquitylation, sumoylation, and others (Huang et al., 2014; Strahl and Allis, 2000; Tan et al., 2011). The PTMs on histones are thought to regulate gene expression through directly affecting chromatin structure and access to DNA, and/or through signaling to and recruitment of other regulatory protein complexes (Kouzarides, 2007; Ruthenburg et al., 2007).

1.2 Regulation of histone methylation

1.2.1 Histone methylation

Methylation of histones occur on basic residues that include arginines, lysines, and histidines (Borun et al., 1972; Byvoet et al., 1972; Murray, 1964). The ε-amine group of lysines can be mono-, di-, or tri-methylated (me1, me2, or me3) (Greer and Shi, 2012; Hempel et al., 1968; Murray, 1964; Paik and Kim, 1967). For arginines, the guanidinyl side chain can be monomethylated or dimethylated symmetrically or asymmetrically (Borun et al., 1972; Byvoet et al., 1972). Although rarely occurring and not as well studied, histidine monomethylation has also been observed (Borun et al., 1972; Gershey et al., 1969). Lysine and arginine methylation on histones H3 and H4 are frequently observed. The more extensively studied lysine methylation residues include H3 lysine 4 (H3K4), H3K9, H3K27, H3K36, H3K79 and H4K20. Arginine methylation is commonly detected at H3R2, H3R8, H3R17, H3R26 and H4R3. Recent advances in mass spectrometry and

quantitative proteomic analyses have identified methylation of numerous other basic residues not only on H3 and H4, but also on histone H1, H2A, and H2B (Young et al., 2010).

1.2.2 Histone methyltransferases (HTMs) and demethylases (HDMs)

The addition of methyl groups from donor S-adenosylmethionine (SAM) to lysine (Murray, 1964) and arginine residues of histones are catalyzed by three families of methyltransferases- the SET-domain-containing proteins, the DOT-1 like proteins, and the protein arginine N-methyltransferase (PRMT) proteins (Bannister and Kouzarides, 2011; Feng et al., 2002; Levine and Yuan, 2005; Murray, 1964). Proteins with a catalytic SET-domain (named after Suppressor of variegation, Enhancer of Zeste, Trithorax (Tschiersch et al., 1994)) are the most common HMTs that methylate many lysine and arginine residues at the N- and C-terminal tails of H3 and H4. Although not as frequent, methylation of the residues in the core globular domain do occur. The non-SET-domain DOT1L protein methylates H3K79. In addition, histone methyltransferases are capable of methylating chromatin-incorporated histones as well as free histones and non-histone proteins (Crooks et al., 2004).

Two types of HDMs function to remove methyl groups from lysines and arginines. The nuclear amine oxidase homologue LSD1 (KDM1A), which demethylates H3K4me1 and me2 and H3K9me2, was the first histone demethylase identified (Shi et al., 2004). The Jumonji-C (JMJC)-domain-containing proteins are iron-dependent oxygenases that constitute most other HDMs (Greer and Shi, 2012; Whetstine et al., 2006). The importance of HMTs and HDMs is underscored by their well-documented associations with various human diseases. Near half of the fifty or so lysine and arginine HMTs have been associated with disease especially with various cancers (Albert and Helin, 2010); and genetic alterations in many JMJC demethylases have been identified in various human neurological disorders and cancers (Park et al., 2016; Pedersen and Helin, 2010).

1.2.3 Targeting of HMTs and HDMs to specific genomic locations

Specific DNA sequences such as Trithorax group (TrxG) and Polycomb group (PcG) response elements identified in *Drosophila* facilitate the recruitment of TRX and Polycomb repressive complex 2 (PRC2) (HMTs for H3K4 and H3K27me3, respectively) to their genomic destinations through transcription factors that bind to these regulatory elements (Chan et al., 1994; Fritsch et al., 1999; Tillib et al., 1999). Long non-coding RNAs (lncRNAs) may also bind to HMTs and HDMs to target the enzymes to specific genomic locations. For instance, lncRNA HOTAIR binds to PRC2 and is required for PRC2 methylation of H3K27me3 at *HOXD* locus (Rinn et al., 2007). In addition, HOTAIR was shown to bind to PRC2 and a LSD1-containing complex, suggesting that lncRNA could coordinate multiple types of methylation (Tsai et al., 2010).

1.3 Consequences of histone methylation

1.3.1 Mechanisms of regulation

There are two established mechanisms for how histone methylation and other PTMs affect chromatin. PTMs can change the overall charge of histones and/or interactions between nucleosomes (Ruthenburg et al., 2007), and as a result, modulate the structure of chromatin and the access of DNA-binding proteins. Alternatively, modified or unmodified histones can recruit proteins with functional domains that recognize and bind to histones. Some modifications may exclude proteins from chromatin. Addition of methyl group increases the hydrophobicity of lysine and arginine residues, and may therefore facilitate hydrophobic interactions with chromatin/DNA binding proteins. Protein domains that can recognize and bind to methylated histones have specific methyl-binding domains such as the chromodomain (Bannister et al., 2001; Lachner et al., 2001), PHD-domain (Shi et al., 2006; Wysocka et al., 2006), or the Tudor domain (Yang et al.,

2010). Changes effected by PTMs in chromatin and binding partners have subsequent impact on downstream biological processes.

1.3.2 Effect of histone methylation

Histone methylation can have different effects on gene expression depending on the residue being methylation and location in the genome. H3K4me3 is located at transcriptionally active genes, but H3K27me3 is a repressive modification (Bernstein et al., 2002; Santos-Rosa et al., 2002). These two antagonizing modifications can be present in same locations, usually at promoters of developmentally important genes. Such regions are called bivalent chromatin, in which the promoters of cell differential genes are kept off but at the same time ready to be activated (Bernstein et al., 2006). In addition, the status of methylation (me1, me2, or me3) is also associated with different outcomes. For instance, H3K79me2 is linked to cell-cycle regulation (Schulze et al., 2009), while H3K79me3 is important for the WNT-signaling pathway (Mohan et al., 2010).

The same type of modification can have opposing effect. H3K4me2-3 can be either transcriptionally active or repressive (Greer and Shi, 2012). Regulation occurs at the level of methyl-binding proteins. H3K4me2-3 are associated with activation (Bernstein et al., 2006), but when they are recognized by the ING2 protein (a PHD-domain-containing co-repressor inhibitor of growth family member 2), the modifications are associated with repressive transcription (Shi et al., 2006). These observations highlight the importance of methyl-binding proteins in determining the outcomes of histone modifications.

1.3.3 Biological consequences of histone methylation

Methylation dynamics of lysine or arginine residues on histone proteins have important roles in many biological processes including essentially all DNA-based processes such as transcription, DNA replication and repair, and chromosome condensation (Kouzarides, 2007). The importance of histone methylation regulation is highlighted by the growing number of links of histone methylation to disease, aging process, and nervous system development. Lower levels of several histone methylation marks are correlated with worse clinical outcomes, poorer survival, or higher recurrence in various cancers (Greer et al., 2010). Balance between activating (H3K4me3) and repressing (H3K27me3) marks are associated with lifespan of multiple organisms, in which levels of HMT and HDM and therefore potentially global methylation level regulate lifespan (Greer et al., 2010; Han and Brunet, 2012; Sen et al., 2016). Individuals with haploinsufficiency in NSD1 or EHMT1 (HMTs for H3K36 and H3K9, respectively) are associated with intellectual disability (Kleefstra et al., 2009; Kurotaki et al., 2002).

1.4 Metabolism and histone methylation

Although histone methylation dynamics is critical to biological processes including gene regulation, most studies have focused on how at specific genomic loci, single or a combination of histone methylation marks may change local chromatin structure or affect the recruitment of regulatory proteins. These localized and specific characterizations do not fully explain how the global levels of histone methylation changes, as observed in cancer tissues, and these changes may result in drastically different clinical outcomes.

Since the cofactors of both HMTs (SAM) and HDMs (FAD or α-ketoglutarate) are important metabolic intermediates (Teperino et al., 2010), it is possible that the global levels of histone methylation may be reflective of the cellular physiological and metabolic states. Metabolism may

influence the regulation of histone methylation through globally produced inhibitory metabolites, site-specific cofactors production, or nutrient sensing (Kinnaird et al., 2016).

1.4.1 How metabolism regulates histone methylation

1.4.1.1 Inhibitor metabolite production

The function of JMJC demethylases depends on α-ketoglutarate (α-KG) (Tsukada et al., 2005), and therefore increased level of structurally similar metabolites may interfere with the cellular usage of α-KG. A number of structurally similar metabolites such as 2-hydroxyglutarate (2-HG), succinate, and fumarate, were reported to be competitive inhibitors of α-KG (Killian et al., 2013; Losman and Kaelin, 2013; Xiao et al., 2012). Tumors lacking succinate dehydrogenase (SDH) or fumarate hydratase (FH) due to mutations accumulate succinate or fumarate, respectively, which inhibit α-KG-dependent enzymes and result in impaired histone demethylation (Xiao et al., 2012). In addition, tumors with mutated isocitrate dehydrogenase (IDH1) were found to produce (R)-2-hydroxyglutarate (R-2HG), which was referred to as the first ‘oncometabolite’ (Dang et al., 2009; Ward et al., 2010). Gliomas containing IDH1 and IDH2 mutations show increased histone H3K9 and H3K27 methylation and abnormal cellular differentiation (Lu et al., 2012).

1.4.1.2 Localized metabolite production

Metabolic enzymes may be recruited to specific sites on chromatin to produce cofactors or subtract locally for chromatin modification. For instance, methionine adenosyltransferase II (MAT2A) is targeted via protein-protein interaction to the DNA binding sites of transcription factor MAFK108 (Katoh et al., 2011). MAT2A can then locally produce SAM for localized H3K9 methylation by HMT SETDB1 (Kera et al., 2013).

1.4.1.3 Nutrient sensing

Chromatin modifications can also occur in direct response to physiological changes in nutrient availability. Such responses may enable cells to optimize crucial short- and long-term adaptation mechanisms in conditions of limited fuel supply, such as those commonly found in many tumors. For instance, the daily intake of essential amino acid methionine (converted into SAM) and folate is essential for the methionine cycle, the levels of SAM and S-adenosylhomocysteine (SAH, SAM transfers methyl to SAH). Thus the level of methylation in tumors may change depending on the diet (Kinnaird et al., 2016; Lim and Song, 2012; Poirier et al., 2001). A more specific example of how nutrient supply can be sensed and affect epigenetic mechanisms is the modulation of SAM and SAH. In cultured cells and *in vivo* in mouse tissues, methionine availability and intracellular production of SAM were shown to directly affect H3K4me3 globally and at specific loci, altering gene transcription (Mentch et al., 2015).

1.5 Significance of the study

Cells respond to environmental challenges such as fluctuating nutrient levels partly through epigenetic mechanisms such as histone modifications and transcriptional regulation to reconfigure their metabolic or physiological states as adaptive measures (Lu and Thompson, 2012; McBrian et al., 2013b; Ye et al., 2017). Understanding the nature and mechanisms underlying cellular response to nutrient availability can inform on fundamental regulatory processes, and how they may be altered in human disease. From among the many nutrients that cells must sense and respond to, amino acids (AAs) are of particular interest because they regulate the mechanistic target of rapamycin complex 1 (mTORC1), a central hub for coordinating cell growth and metabolism (Saxton and Sabatini, 2017). Although considerable progress has been made in recent years about how AAs activate mTORC1 and its downstream effects (Goberdhan et al., 2016), much less is known about the epigenetic changes that may be required,

especially independently of mTOR signaling, for effective adaptive response to limited AA availability.

We examined how global levels of histone methylation change in response to availability of various nutrients of the tissue culture medium and what functional role the changes play in gene regulation. We found that as a result of amino acid starvation and impaired translation, H4K20me1 is reduced genome wide from the gene body, where it is normally enriched. In addition, the decrease of H4K20me1 is marked by a corresponding genome wide increase of MYC binding. The increased MYC binding is most significant in a group of upregulated genes encoding translation initiation factors and ribosomal proteins (RPs). We demonstrated that both the loss of H4K20me1 and the gain of MYC are necessary for the upregulation of these genes to prepare the cells for recovery of translation initiation once amino acid availability is restored. Our data reveal a novel connection between translational state of the cell and chromatin and transcriptional regulation.

CHAPTER 2

Results

2.1 Availability of amino acids affects global level of H4K20me1

We first asked if any of the components in cell culture Dulbecco's Modified Eagle's medium (DMEM) affects global levels of histone methylation. HeLa cells were cultured for 16 hours in complete medium or media lacking DMEM components, which include vitamins, glucose, pyruvate, and amino acids (AAs). Removal of all 15 AAs, but none of the other media components, significantly reduced levels of H4K20me1 (Figure 1A). The effect of AA availability appeared to be specific to H4K20me1, as the methylation of other lysine residues on histone H3 and H4 is not affected (Figure 1B).

To determine which if any of the 15 amino acids is essential for the effect on H4K20me1, HeLa cells were cultured in media lacking groups of AAs. Eliminating all the essential amino acids (EAA) or the non-essential amino acids (NEAA) caused only minor reduction of H4K20me1 (Figure 1C). In addition, when cells were provided with media containing varying amount of the 15 AAs, level of H4K20me1 was reduced in a dose dependent manner (Figure 1D). We conclude that the global level of H4K20me1 varies proportionally to the overall available pool of AAs rather than to specific amino acids.

The effect of AA restriction on H4K20me1 is reversible and conserved between cancer and normal cell types. In the absence of AAs, the cells remained viable over the course of the experiment (Figure 2A) and recovered H4K20 monomethylation when AAs were added back (Figure 2B). We confirmed the effect of AA deprivation on global H4K20me1 in HeLa cells with a different antibody (Figure 2C) and observed the same effect in normal human bronchial/tracheal epithelial cells (HBTEC) and primary fetal lung fibroblasts (IMR90) (Figure 2D).

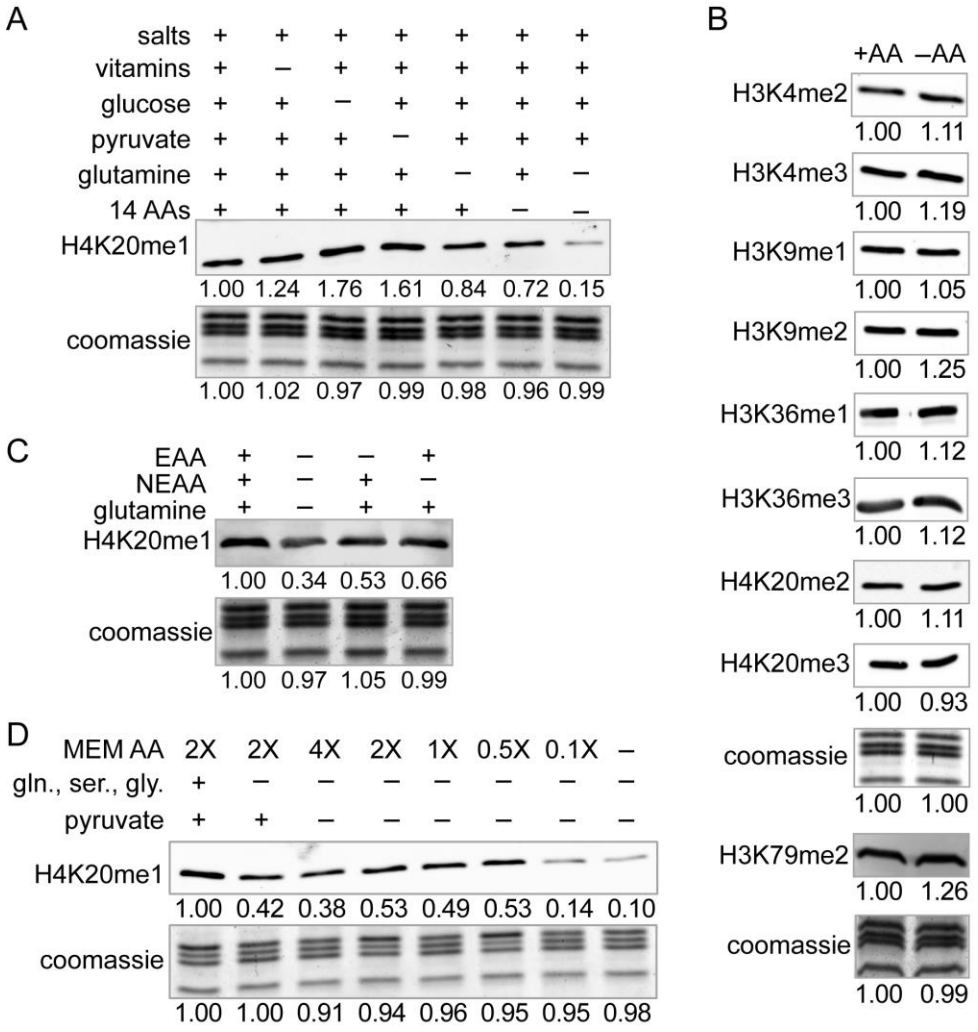

Figure 1. Global level of H4K20me1 varies proportionally to amino acid availability

(A) Western blotting (WB) of H4K20me1 in cells cultured for 16 hours in media lacking components of DMEM as indicated. 14AA, the 14 non-glutamine amino acids in DMEM; coomassie, the relative amounts of total histones loaded.

(B) WBs of histone methylation of cells cultured with (+AA) or without (–AA) amino acids for 16 hrs. The same preparation of histones was used to perform all WBs in this figure except for H3K79me2, which was done at a later time with its own loading control (bottom panel).

(C) WB of H4K20me1 in cells cultured in media lacking groups of AA as indicated. EAA, essential amino acids; NEAA, non-essential amino acids.

(D) WB of H4K20me1 in cells cultured in different amount of amino acids. MEM AA mixture is approximately 0.5X of DMEM AA and does not include glutamine, serine, and glycine. A mixture of 2X MEM plus Gln, Ser, and Gly (i.e., lane 1) is the approximate equivalent of AA concentration in standard DMEM.

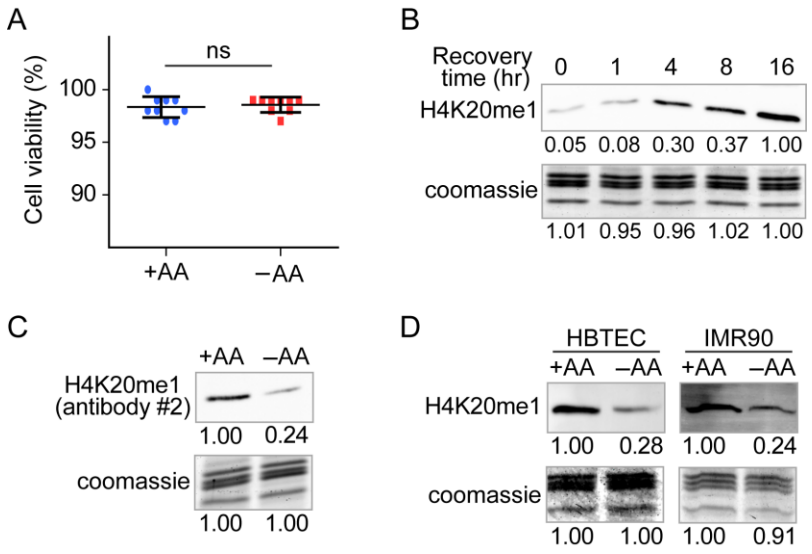

Figure 2. The effect of AA restriction on H4K20me1 is reversible and conserved in different cell types

(A) Viability of cells cultured in +AA or –AA using Trypan Blue staining. ns, not significant.

(B) WB of H4K20me1 in cells cultured without (–AA) amino acids for 16 hrs followed by recovery in complete media with AA for the indicated time.

(C) WBs of H4K20me1 using a second antibody (Active Motif cat. no. 39175; lot no. 01008001) in HeLa cells cultured with (+AA) or without (-AA) amino acids. (Note that the Abcam H4K20me1 antibody (cat. no. 9051; lot no. GR79450-1) was used for all other WB and ChIP experiments in this study.)

(D) WBs of H4K20me1 in normal human bronchial/tracheal epithelial cells (HBTEC) or primary fetal lung fibroblasts (IMR90) cells cultured with (+AA) or without (-AA) amino acids.

2.2 Cellular translational capacity affects global level of H4K20me1

Eukaryotic cells integrate various environmental cues including amino acid through the mTORC1 signaling pathway (Jewell et al., 2013). As expected, removal of AAs inhibited mTORC1 activity as measured by its ability to phosphorylate S6K (Figure 3A). However, inhibiting mTORC1 activity with Rapamycin did not reduce the level of H4K20me1 (Figure 3B). This observation indicates H4K20me1 is affected by AA availability in parallel to deactivation of mTORC1 signaling.

Since AA availability affects rate of protein synthesis (Pain, 1994), we asked whether inhibition of translation in presence of AAs also affects H4K20me1. HeLa cells were cultured in

complete DMEM media with the addition of protein translational inhibitor cycloheximide (CHX). The level of H4K20me1 decreased with increasing amount of CHX (Figure 3C), which suggests that H4K20me1 level is sensitive to the translation capacity of the cells and not AA availability per se.

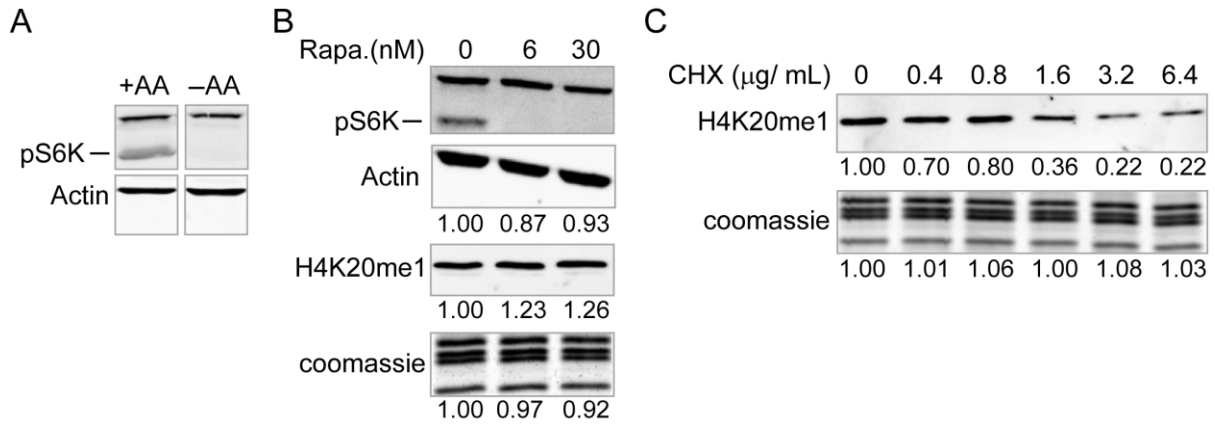

Figure 3. The effect of AA restriction on H4K20me1 is independent of mTOR signaling and associated with translation capacity

(A) WBs of phospho-S6K of cells cultured in +AA or –AA.

(B) WBs of phospho-S6K and H4K20me1 of cells treated with Rapamycin (Rapa.) or DMSO (0 nM) in complete DMEM.

(C) WB of H4K20me1 in cells treated with the indicated amount of cycloheximide (CHX) or DMSO (0 μg/mL) in complete DMEM.

2.3 AA-dependent change in H4K20me1 level correlates with levels of SETD8 HMT

H4K20me1 methyltransferase SETD8 (Pr-SET7) level varies during cell cycle progression, with lowest level in S phase but increases to maximal level in late G2 (Rice et al., 2002; Wu et al., 2010). We asked whether AA/translation-dependent change of H4K20me1 is related to SETD8 level and/or cell cycle stage. The level of SETD8 reduced in cells cultured in media lacking amino acids (Figure 4A), which suggests AA-dependent H4K20me1 change is mediated through SETD8 turnover. However, SETD8 turnover in this case appears to be independent of cell cycle progression, since flow cytometry measurement of propidium iodide (PI) stained cells showed

that cell cycle profile did not change significantly in cells cultured without AAs (Figure 4B). Similarly, inhibition of protein synthesis, while resulted in a reduction of H4K20me1 (Figure 3C), had no appreciable effect on the cell cycle profile assessed by PI staining of DNA contents (Figure 4C). Therefore, AA/translation-dependent change in H4K20me1 levels is associated with SETD8 turnover, and is not a secondary consequence of cell cycle changes.

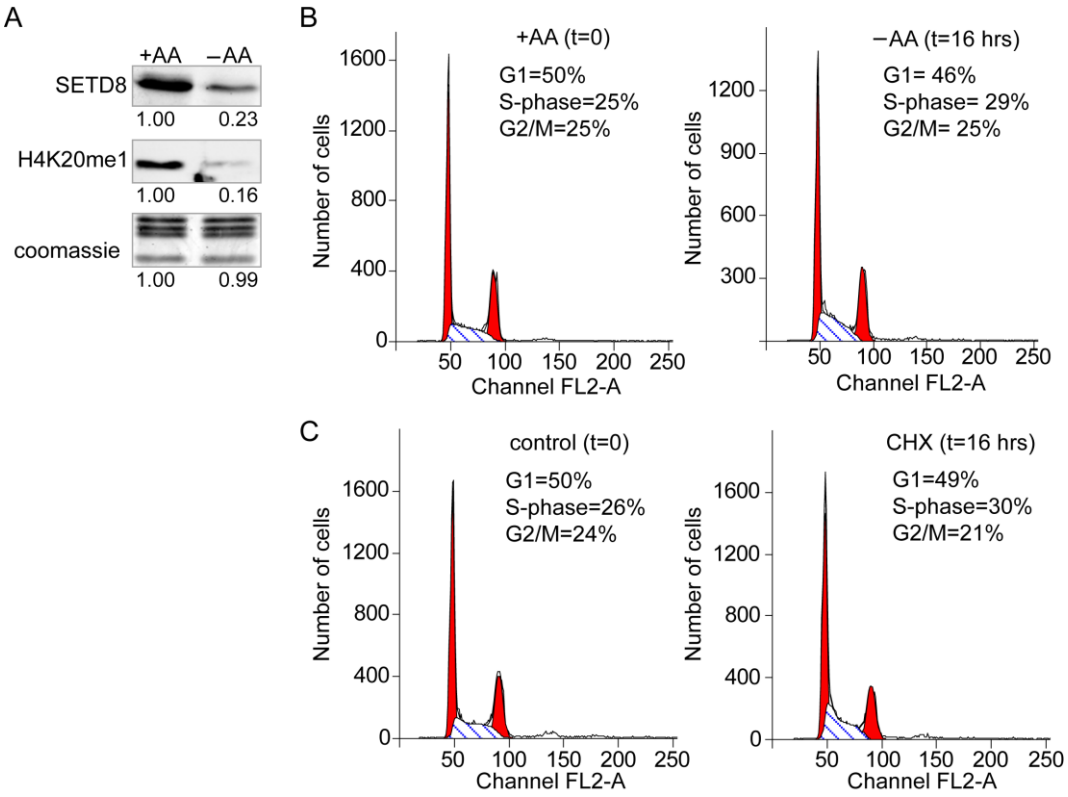

Figure 4. AA-dependent H4K20me1 change is mediated through methyltransferase but independent of cell cycle progression

(A) WBs of H4K20me1 and SETD8 in cells cultured with (+AA) or without (–AA) amino acids.

(B-C) Flow cytometry analysis of propidium iodine (PI) stained HeLa cells cultured in the indicated conditions. The percentage of cells in each phase of the cell cycle is indicated.

2.4 Demthylation is involved in AA-dependent H4K20me1 change

We asked whether the effect of AA restriction on H4K20me1 reduction could be prevented by inhibiting SETD8 turnover. Inhibitor of proteasome 26S complex, MG132, was used to reduce the degradation of ubiquitin-conjugated proteins (Lee and Goldberg, 1996; Rock et al., 1994). While addition of MG132 prevented substantial reduction of SETD8 level in cells cultured in media lacking AAs, it did not prevent H4K20me1 reduction (Figure 5A). These results indicate that AA-dependent H4K20me1 change is mediated through a mechanism involves both methyltransferase SETD8 and an unknown demethylase. We confirmed the effect of demethylation with a targeted knockdown of Cdt2, the E3 ligase of SETD8 (Abbas et al., 2010). Similar to MG132 treatment, Cdt2 knockdown, while stabilize the degradation of SETD8 in the absence of AAs, did not prevent H4K20me1 reduction (Figure 5B). Furthermore, since acute AA restriction triggers proteasomal protein degradation to supply amino acids for protein synthesis (Vabulas and Hartl, 2005), in MG132 treatments, the cellular pool of AAs is likely reduced due to proteasome inhibition. Therefore it makes sense that in MG132 treated cells, global H4K20me1 was reduced to a level lower than cells treated with control DMSO (Figure 5A); and MG132 treatment resulted in H4K20me1 reduction even in the presence of AAs (Figure 5C).

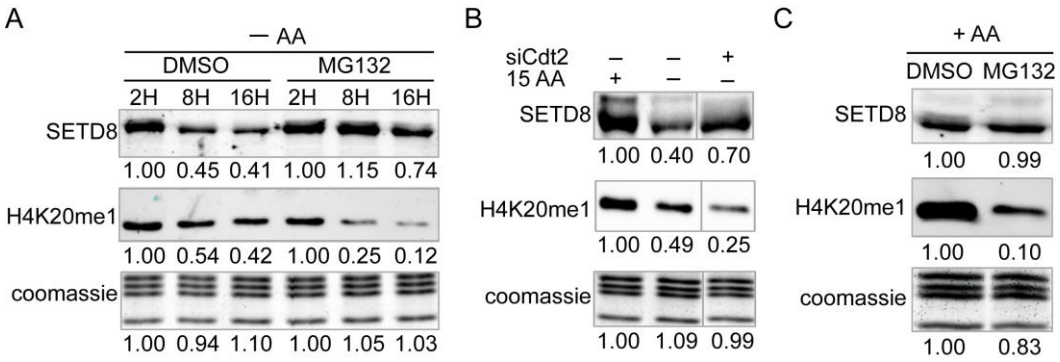

Figure 5. Demthylation has a role in AA-dependent H4K20me1 change

(A) WBs of SETD8 and H4K20me1 in cells cultured in media lacking amino acids (–AA) with the addition of DMSO or MG132.

(B) WBs of SETD8 and H4K20me1 in cells treated with mock transfection or Cdt2 knockdown and cultured in media with (+AA) or without (–AA) amino acids.

(C) WBs of SETD8 and H4K20me1 in cells cultured in complete media (+AA) with the addition of DMSO or MG132.

2.5 AA-dependent change of H4K20m1 is genome-wide

To determine how the AA-dependent changes in global level of H4K20me1 map to specific genomic loci, we performed chromatin immunoprecipitation sequencing (ChIP-seq) analysis in cells in presence or absence of amino acids. H4K20me1 was enriched primarily in the gene bodies of 7589 genes (Figures 6A-6B). A gene is considered as H4K20me1 associated if there is significant enrichment within the -1 to +5 kb region around transcription start site (TSS). The level of H4K20me1 was reduced in vast majority of the genes with greater than 95% genes exhibiting decreasing level of H4K20me1 (Figures 6A-6B). The most significantly enriched gene ontology (GO) terms for H4K20me1-associated genes include those involved in protein homeostasis such as rRNA-processing, translational initiation, nonsense mediated decay, and co-translational targeting (Figures 6C).

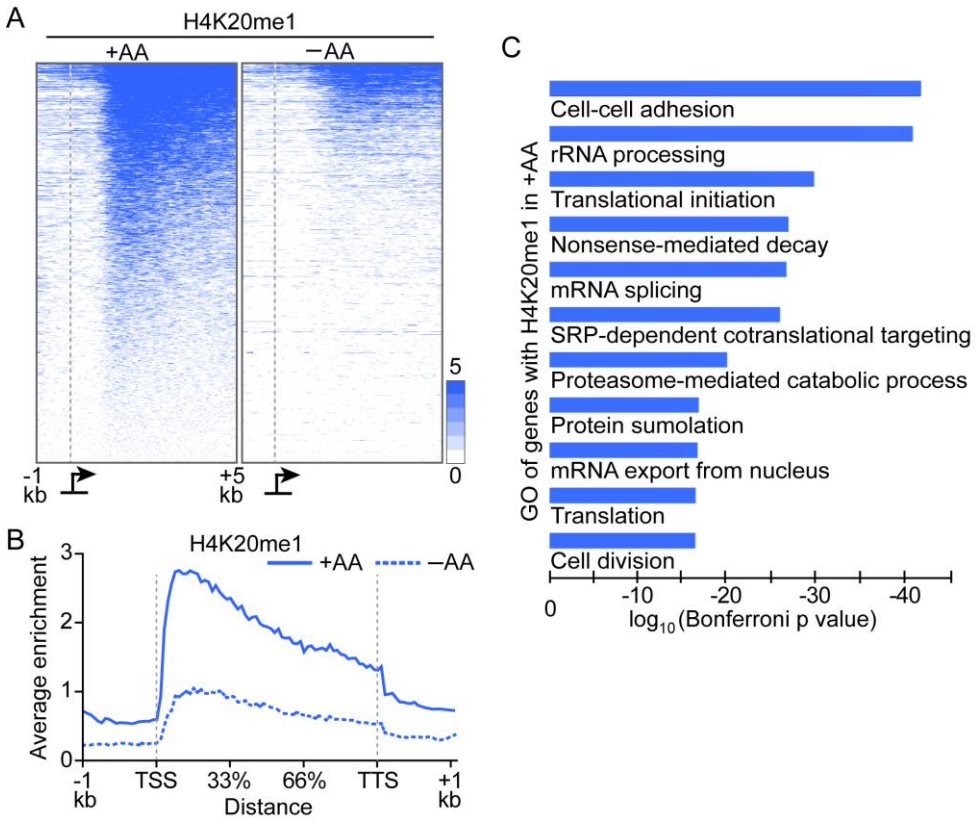

Figure 6. Amino acid restriction induces loss of H4K20me1 from gene bodies

(A) Heat maps showing the distribution of significant peaks of H4K20me1 in the indicated media within the region -1 to +5 kb around the transcription start site (TSS). Included in the heat maps are all the genes with significant H4K20me1 enrichment within the 6-kb region in +AA. TTS, transcription termination site.

(B) Metagene plot of H4K20me1 levels for genes in (A) scaled to a distance of 3-kb between transcription start and termination sites. The distances away from the gene body are not scaled.

(C) Gene ontology (GO) analysis of H4K20me1 associated genes from (A).

Consistent with the Western blot results (Figure 1B), genome-wide distribution of H3K36me3, which is also enriched in the gene body, did not change substantially (Figures 7A-7B); confirming that AA restriction preferentially affects H4K20me1. The decrease in H4K20me1 did not appear to be due to increasing di- or tri-methylation of the same residue as the global levels of H4K20me2 and me3 were unaffected in the absence of AAs (Figure 1B), and more importantly, H4K20me3 genome-wide enrichment pattern is physically distinct from H4K20me1 (Figure 7C).

.

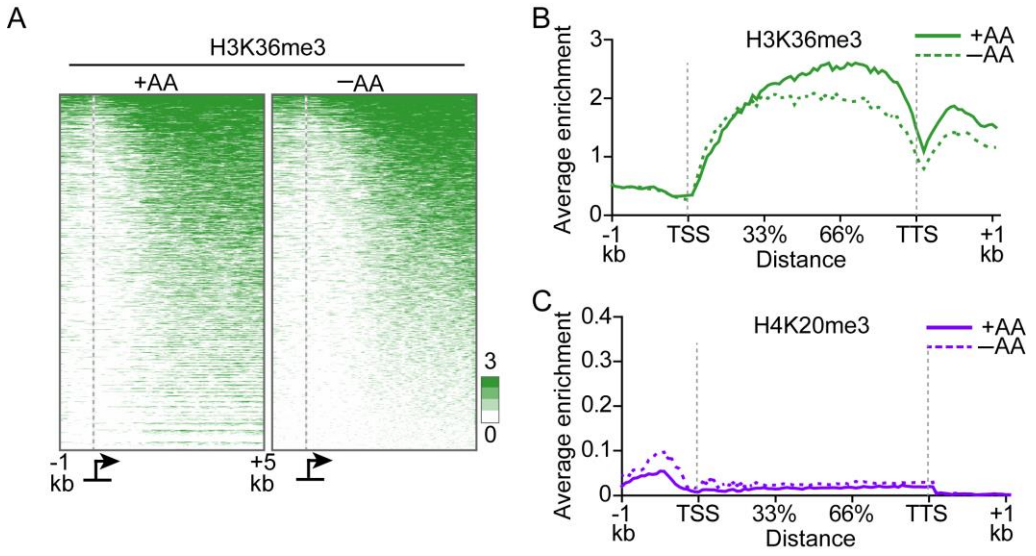

Figure 7. Amino acid restriction did not substantially affect H3K36me3 or H4K20me3 genome-wide

(A) Heat maps showing the distribution of significant peaks of H3K36me3 in the indicated media within the region -1 to +5 kb around the transcription start site (TSS). Included in the heat maps are all the genes with significant H3K36me3 enrichment within the 6-kb region in +AA.

(B) Metagene plot of H3K36me3 levels for genes in (A) scaled to a distance of 3-kb between transcription start and termination sites. The distances away from the gene body are not scaled.

(C) Metagene plot of H4K20me3 levels for H4K20me1-associated genes shown in Figures 6A-6B scaled to a distance of 3-kb between transcription start and termination sites. The distances away from the gene body are not scaled.

2.6 Genes with reduced level of H4K20me1 and involved in translational initiation are transcriptionally upregulated

To correlate changes in H4K20me1 to gene expression, we performed mRNA-seq with a spike-in control in the same conditions as in ChIP-seq experiments. Compared to complete media, of all H4K20me1-associated genes, 966 and 744 were up- and down-regulated greater than 1.5-fold, respectively, in media lacking AAs (Figure 8A, left panel). The genes within the upregulated group had the greatest loss of H4K20me1 (Figure 8B) and were significantly enriched for genes involved in translation-related processes (Figure 8A, right panel, orange bars). In contrast, the downregulated genes were only marginally enriched in specific GO terms (Figure 8A, right panel, green bars). A closer analysis of the top GO terms among the upregulated genes (Figure 8A) (i.e., translational initiation, co-translational targeting, rRNA-processing, nonsense mediated decay, and translation) revealed a common set of genes encoding translation initiation factors (EIFs) and large and small ribosomal proteins (RPs).

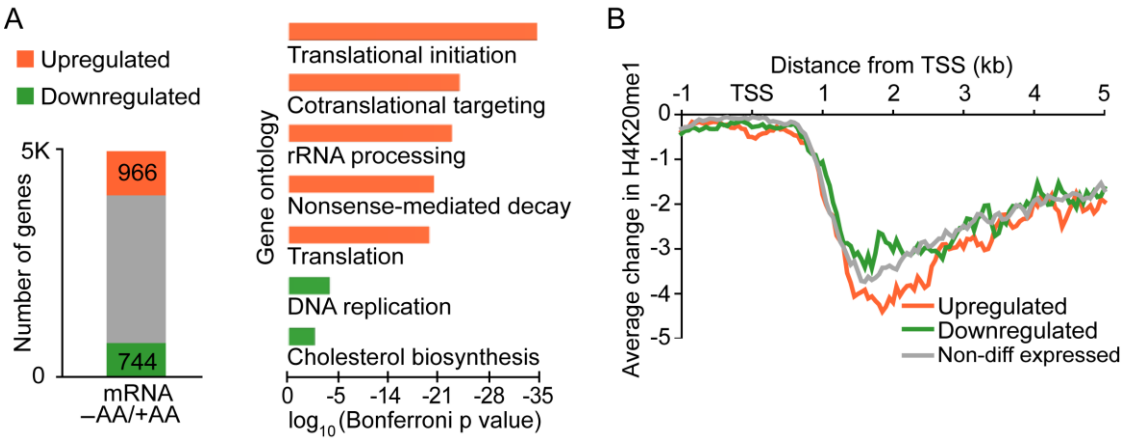

Figure 8. AA-dependent H4K20me1 loss correlates with upregulation of genes involved in translation.

(A) Left panel, numbers of genes with mRNA upregulated or downregulated greater than 1.5-fold in –AA compared to +AA. Right panel, GO analysis of upregulated or downregulated genes.

(B) Average differential enrichment of H4K20me1 (–AA vs. +AA) within the region -1 to +5 kb around TSS from upregulated, downregulated, or non-differentially expressed genes (as identified in Figure 8A).

To determine whether differentially expressed genes were regulated at the level of transcription, we mapped the levels of total RNA polymerase II (Pol II) and elongating phospho-Ser2 Pol II (Ser2P), as well as RNA-seq of the chromatin fraction (chromRNA-seq), representing newly synthesized transcripts. The upregulated genes based on mRNA-seq had higher Pol II enrichment in both the promoter proximal region and gene body in the condition lacking AAs (Figures 9A-9B, left panels). In contrast, there were no marked differences in Pol II occupancy between the two conditions among the downregulated genes (Figures 9A-9B, right panels). Consistent with Pol II occupancy and mRNA-seq, chromRNA-seq showed increased nascent RNA associated with the upregulated but not with the downregulated genes (Figures 9C-9D). These data indicate that genes with increased mRNA levels because of AA deficiency are upregulated transcriptionally.

A second biological replicate of mRNA-seq experiment, without a spike-in control, showed essentially identical functional enrichment of up- and down-regulated genes (Figure 10A). In addition, we asked whether normal primary cell lines also upregulate translation initiation genes in response to absence of amino acids. RNA-seq experiments were performed in normal bronchial/ tracheal epithelial cells (HBTEC) and primary lung fibroblast (IMR90) in the same conditions of with or without AAs. HBTEC and IMR90 cells also upregulated translation-related genes (Figure 10B). In fact, the upregulated genes common to all three cell lines were highly significantly enriched with translational initiation and rRNA processing factors as well as RP genes (Figure 10C).

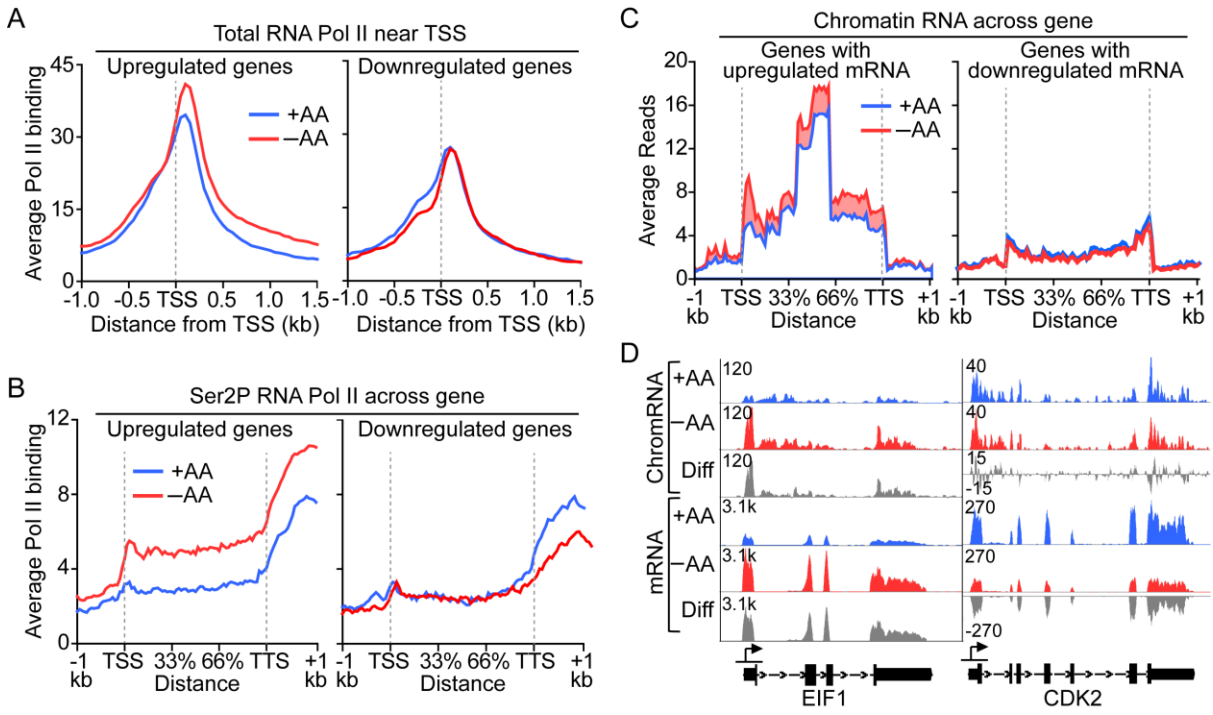

Figure 9. Upregulated genes are regulated transcriptionally

(A) Average significant enrichment of total RNA Pol II within the region -1 to +1.5 kb around the TSS of the upregulated or downregulated genes shown in Figure 8.

(B) Metagene plots of significant Ser2P RNA Pol II enrichment of the upregulated or downregulated genes shown in Figure 8. The enrichment profiles were scaled to a distance of 3-kb between transcription start and termination sites. The distances away from the gene body are not scaled.

(C) Metagene plot showing chromatin fraction RNA-seq (chromRNA) coverage of the upregulated or downregulated group of genes shown in Figure 8. The RNA-seq coverage profiles were scaled to a distance of 3-kb between transcription start and termination sites. The distances away from the gene body are not scaled.

(D) Genome browser tracks showing chromRNA and mRNA coverage in +AA and –AA from representative upregulated or downregulated genes shown in Figure 8.

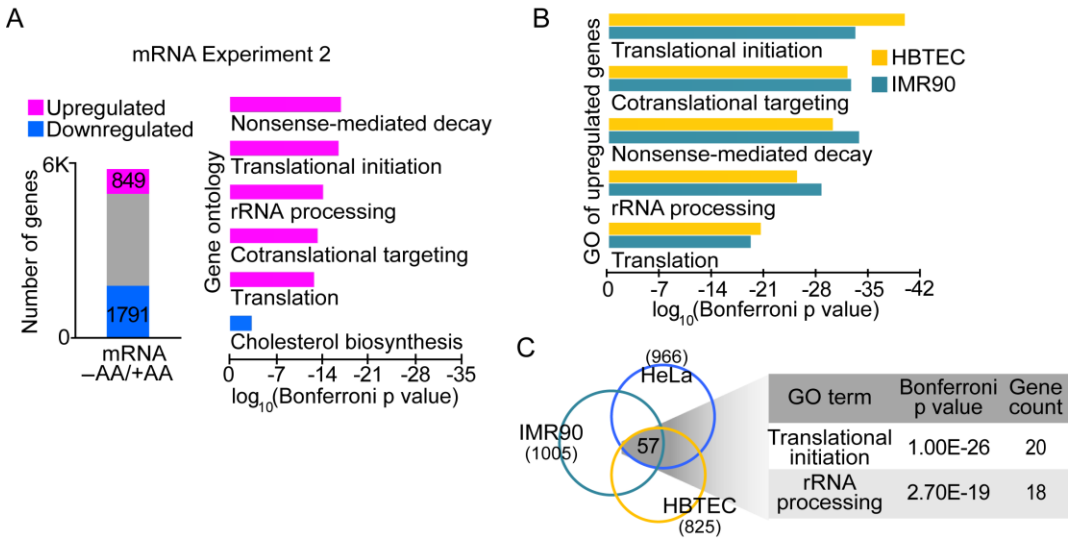

Figure 10. Transcriptional regulation of AA restriction is conserved in different cell types

(A) Related to Figure 8A. Biological replicates of mRNA-seq of HeLa cells cultured in +AA or –AA without a spike-in control. Left panel, numbers of genes with mRNA upregulated or downregulated greater than 1.5-fold in –AA compared to +AA. Right panel, GO analysis of upregulated or downregulated genes.

(B) GO analysis of upregulated genes in –AA vs. +AA from normal primary IMR90 and HBTEC cells.

(C) The number of commonly upregulated genes in –AA and their GO analysis from the indicated cell types.

2.7 Genome-wide binding of MYC increases in response to lack of AAs

We asked how genes are transcriptionally upregulated as a result of reduced genic H4K20me1. We noticed that the promoter proximal sequences of the upregulated set of translational initiation genes are enriched with binding motif for transcription activator MYC and its binding partner MAX (Figures 11A); and the expression of Myc mRNA is upregulated in the absence of AAs (Figures 11B). We therefore examined the binding of MYC by ChIP-seq analysis and found a substantial and genome-wide gain of MYC binding in the absence of AAs (Figures 11C-11D).

Interestingly, there was a significantly greater increase in MYC binding within 1 kb of transcription start sites (TSS) of the H4K20me1 associated genes belonging to the GO terms “translational initiation” and “rRNA processing” which include EIFs and RPs genes (from Figure 6C, n=217 genes) compared to randomly selected (100 permutations) sets of genes not in those terms (Figure 12A). A closer observation of ChIP-seq enrichment at specific genes revealed that upregulated translational initiation genes are marked with a corresponding H4K20me1 decrease (Figures 12B). These observations suggested that in response to lack of AAs and impaired translation, translational initiation genes are targeted for upregulation perhaps through a combination of H4K20me1 loss and MYC binding gain.

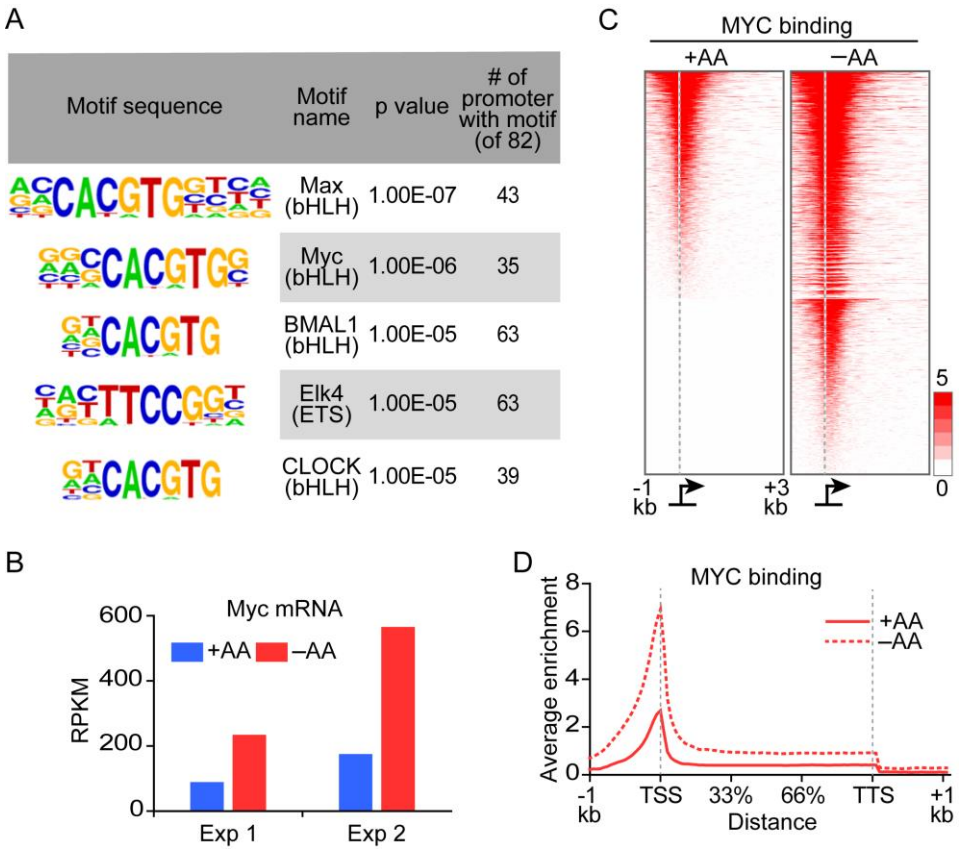

Figure 11. Amino acid restriction induces MYC binding genome-wide

(A) Motif enrichment analysis of the promoters of upregulated genes involved in translational initiation and rRNA processing as shown in figure 6C. Regions from -500 to +750 bp of each promoter sequence were used for analysis.

(B) Bar graphs showing upregulation of Myc mRNA in –AA compared to +AA from two independent RNA-seq experiments.

(C) Heat maps showing the distribution of significant peaks of MYC binding in the indicated media for all the genes with significant MYC binding enrichment within the -1 to +3 kb region in +AA or –AA.

(D) Metagene plot showing significant enrichment of MYC binding in the same group of genes shown in figure 11C. The enrichment profiles were scaled to a distance of 3-kb between transcription start and termination sites. The distances away from the gene body are not scaled.

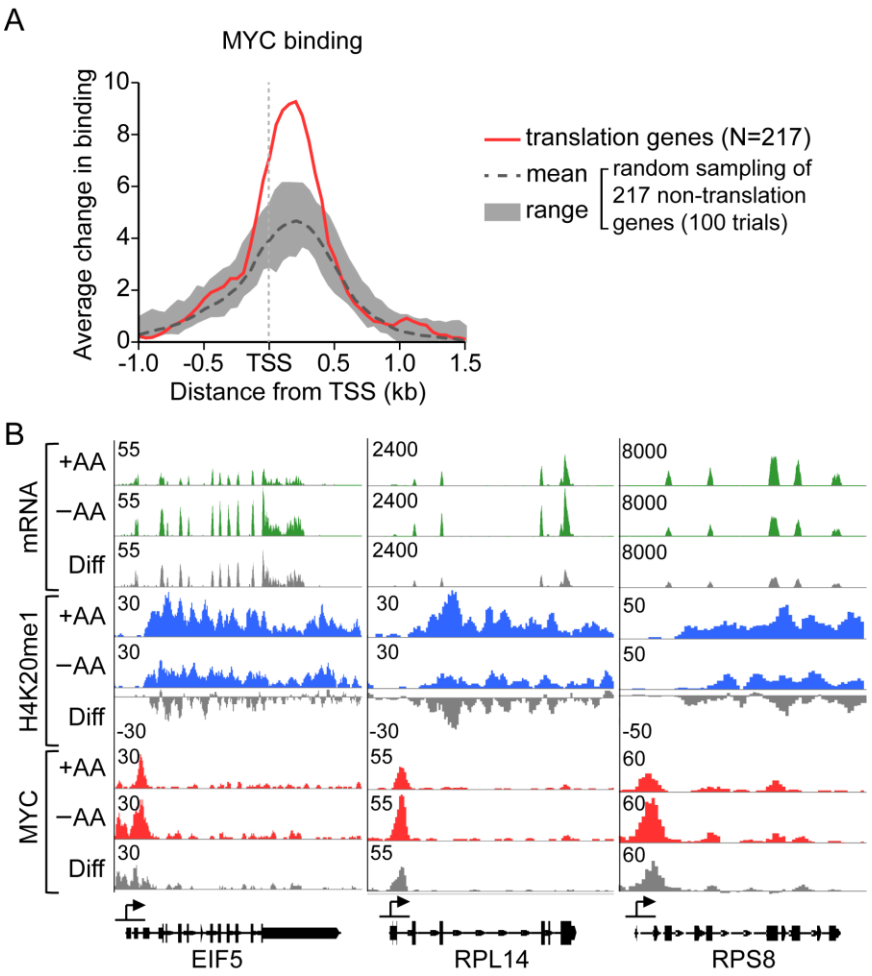

Figure 12. Amino acid restriction increases MYC binding preferentially at genes involved in translation

(A) Average differential binding of MYC around TSS of genes involved in translation (in red) or a group of randomly sampled non-translation related genes. The shaded grey and dashed line show the range and the mean of values from 100 sampling trials.

(B) Genome browser tracks of representative translation initiation factor and large and small ribosomal protein genes. Diff, the difference in significant enrichment (H4K20me1 and MYC) or mRNA-seq coverage between the two condition (subtract +AA from –AA).

2.8 Lose of H4K20me1 and gain of MYC binding are both needed to upregulate ribosomal proteins

To determine whether loss of H4K20me1 and gain of MYC binding are required to upregulate the expression of translation-related genes, we recapitulated these events in presence of AAs. We first knocked down *Setd8*, which effectively decreased H4K20me1 to a level similar to removal of AAs and which had no effect on MYC expression (Figure 13A). Ectopic overexpression of MYC did not affect H4K20me1 level (Figure 13B). We then performed RNA-seq experiments in these conditions. The mRNA expression differences were compared between a treatment condition and its corresponding control for all translation initiation factors (EIFs) and ribosomal proteins (RPs) found to lose H4K20me1 without AAs (i.e., those shown in Figure 6C). RNA-seq data showed that Setd8 knockdown does not significantly affect the mRNA expression of the EIFs or RPs (Figure 13C). When only MYC is elevated, the mRNAs of several initiation factors are increased; however, transcripts abundance of most large and small ribosomal components was not affected (RPLs and RPSs). However, concurrent knockdown of Setd8 and overexpression of MYC resulted in increased expression of most initiation factors and ribosomal proteins (Figure 13C). We conclude that a combination of H4K20me1 loss and MYC gain in the translational initiation genes are required to upregulate their expression in response to impaired protein translation capacity.

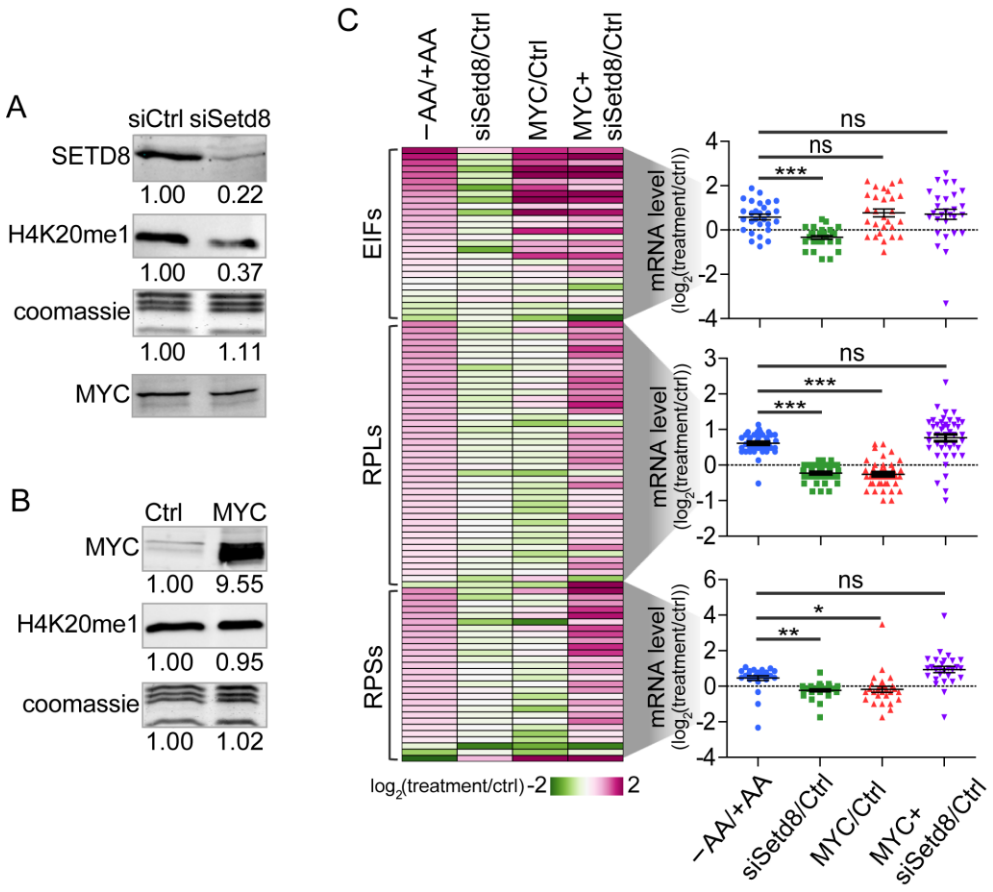

Figure 13. Concurrent loss of H4K20me1 and MYC overexpression are necessary for the transcriptional upregulation of translational initiation and protein synthesis

(A) WBs of SETD8, H4K20me1, and MYC in control and Setd8 knockdown.

(B) WBs of MYC and H4K20me1 in control and MYC overexpression.

(C) Expression levels (heat map) and distributions (dot plots) of translation related genes in the indicated conditions. The Student's paired t-test with a two-tailed distribution was used to calculate P values. ***P<0.0001, **P<0.001, *P<0.5, ns, not significant. Values shown in the heat map are listed in Table 5-1.

2.9 Upregulation of translational genes leads to increased protein synthesis

Since depletion of amino acids from culture media reduces overall protein synthesis (van Venrooij et al., 1972), we asked whether the upregulation of translation related genes is functionally relevant. Cells were cultured for 16 hours with or without AAs, and subjected to pulse-labeling in

DMEM with or without AAs but supplemented with [^{35}S]-labeled methionine and cysteine. Whole cell lysates were precipitated with trichloroacetic acid (TCA) to monitor the incorporation of radioactivity into total cellular proteins. After 30 or 60 minutes of labeling, cells cultured without AAs prior to and during labeling showed significantly less incorporation as would be predicted by depletion of the cellular AA pool (Figure 14A). Importantly, however, cells cultured without AAs prior to labeling but with full complement of AAs during labeling had significantly more incorporation of [^{35}S]-labeled methionine/cysteine than those continuously cultured in complete media (Figure 14B). These observations were confirmed in primary fetal lung fibroblasts (IMR90) (Figure 14C); and together indicate that when AAs become limiting, a subset of RP and translation initiation genes are upregulated and translation capacity is increased.

The baseline translation capacity in rich media and its elevated level in response to the absence of amino acids were dependent partly on the function of MYC. Cells cultured in presence of the MYC inhibitor 10058-F4, which antagonizes MYC binding to DNA (Yin et al., 2003), for 8 hours prior to [35S] labeling, had significantly lower protein synthesis (Figure 15). Interestingly, the MYC inhibitor was more effective at inhibiting protein synthesis when cells were cultured in the presence of AAs than in their absence (Figure 15A). This is consistent with increased expression and binding of MYC under AA deprivation condition (Figure 11), which may render the inhibitor drug less effective at inactivating MYC. However, just as overexpression of MYC alone was insufficient to fully induce the expression of translation-related genes (Figure 13C), it also did not increase protein synthesis in rich media (Figure 16A). Finally, and importantly, concurrent knockdown of Setd8 and overexpression of MYC resulted in increased synthetic capacity in rich media (Figure 16B). We therefore conclude that MYC and H4K20me1 coordinately regulate the expression of a subset of translation-related genes, modulating translational capacity in response to availability of AAs or productive translation.

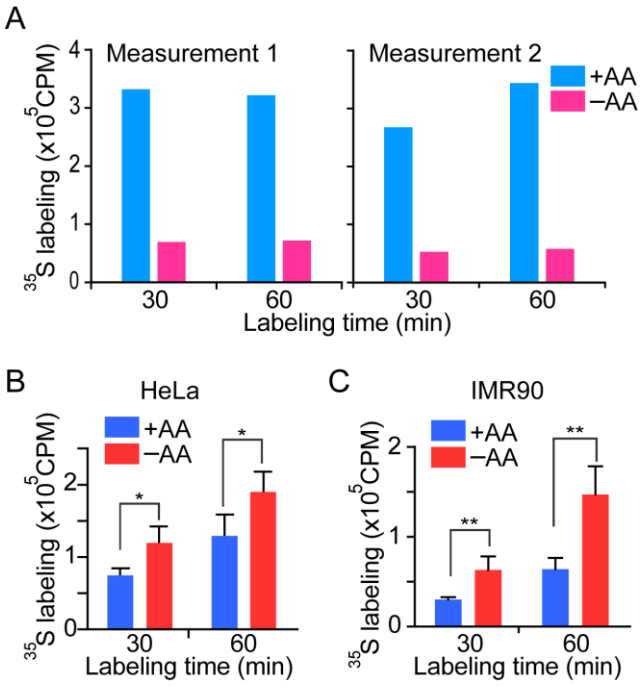

Figure 14. Protein synthesis capacity increases because of upregulated initiation factors and ribosomal proteins

(A) Levels of [35S]-methionine/cystiene incorporation by cells cultured in +AA or –AA for 16 hours prior to pulse labeling. In this experiment, –AA labeling medium contained only [35S]-methionine/cystiene with no additional amino acids to force the cells to rely on the internal pool of AAs for protein synthesis.

(B) Levels of [35S]-methionine/cystiene incorporation by HeLa cells cultured with or without amino acids prior to pulse labeling. Student's paired t-test with a two-tailed distribution, *P<0.01, N=9.

(C) Levels of [35S]-methionine/cystiene incorporation by IMR90 cells cultured with or without amino acids prior to pulse labeling. Student's paired t-test with a two-tailed distribution, ** P<0.001, N=9

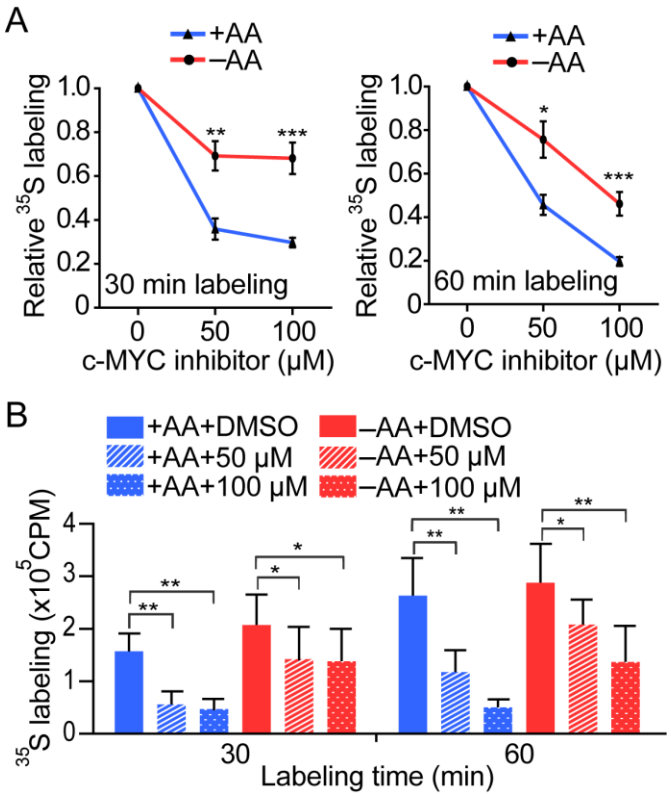

Figure 15. Effect of MYC binding on protein synthesis

(A) Relative levels of [35S]-methionine/cystiene incorporation by cells treated with DMSO or indicated concentrations of MYC inhibitor 10058-F4 prior to pulse labeling. Student's paired t-test with a two-tailed distribution, *P<0.05, **P<0.01, *** P<0.001. N=9.

(B) Primary data for Figure 15A. Levels of [35S]-methionine/cystiene incorporation by cells treated with DMSO or indicated concentrations of MYC inhibitor 10058-F4 prior to pulse labeling. [35S]-methionine/cystiene labeling was done with the full complement of amino acids. Student's paired t-test with a two-tailed distribution, *P<0.01, **P<0.0001. N=9

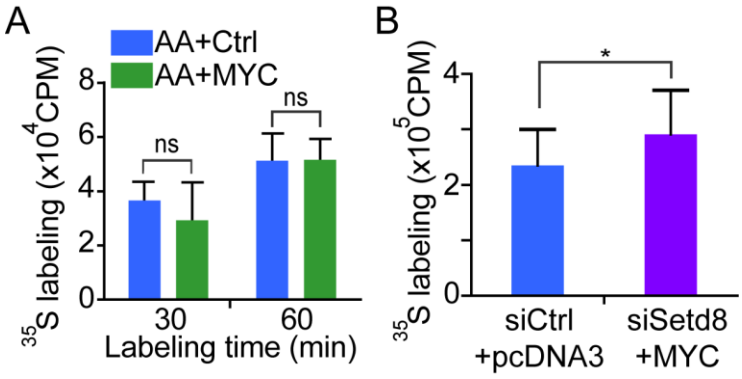

Figure 16. Concurrent loss of H4K20me1 and MYC overexpression are necessary for enhanced protein synthesis

(A) Levels of [35S]-methionine/cystiene incorporation by cells cultured in +AA and transfected with control or MYC expression plasmids for 48 hrs prior to pulse labeling. ns, not significant.

(B) Levels of [35S]-methionine/cystiene incorporation by cells cultured in +AA and transfected with indicated siRNA and expression plasmid prior to pulse labeling. Student's paired t-test with a two-tailed distribution, *P<0.01.

CHAPTER 3

Discussion

We presented in this study evidence supporting H4K20me1 as an epigenetic mark that enables cells to links the state of protein synthetic capacity to the transcriptional machinery. H4K20me1 may normally, under nutrient rich environment, act as a brake for excessive transcription. In response to limited availability of AAs or impaired cellular translation capacity, H4K20me1 decreases which together with increased MYC binding transcriptionally activate the genes necessary for translation re-initiation upon recovery of nutrient.

3.1 H4K20me1 in transcriptional activation and repression

H4K20me1 and SETD8 function both during active transcription and transcriptional repression. PR-Set7/SETD8 was initially isolated in *Drosophila* to be associated with silent chromatin and does not localize with elongating Ser2P RNA Pol II (Nishioka et al., 2002). In undifferentiated mouse ES cells, H4K20me1 is associated with the initiation of X inactivation (Kohlmaier et al., 2004). In contrast, bivalent genes that lose H3K27me3 and become activated after differentiation are associated with increased levels of H4K20me1 and RNA polymerase II in multipotent human primary hematopoietic stem cells/progenitor cells (Cui et al., 2009). Similar to our observation in HeLa cells, in T lymphocytes, H4K20me1 peaks were found to localize downstream from the TSS and to highly correlate with active transcription (Barski et al., 2007; Wang et al., 2008). It has also been suggested that H4K20me1 promotes transcriptional repression by transition to H4K20me3, which has a well-studied role in gene repression (Beck et al., 2012; Schotta et al., 2004; Schotta et al., 2008). The repressive function via H4K20me3 if any is likely indirect, since we as well as others observed that H4K20me1 and me3 occur in different regions of the genome; and that loss of H4K20me1 is not due to conversion to H4K20me3. H4K20me1 peaks were found to localize downstream from the TSS, while H4K20me3 peaks are associated with repetitive regions and promoters (Figure 7C) (Congdon et al., 2010). In our conditions, H4K20me1 appears to play an inhibitory role for translation-related genes.

3.2 Regulation of H4K20me1 by demethylation

Exactly how H4K20me1 is regulated in response to AA restriction, whether its loss in the absence of AAs is due to passive or active demethylation or a combination of both, remains a question. H4K20me1 has a half-life of ~9 hours (Zee et al., 2010), suggesting that in principle some loss of methylation could occur passively in the course of our experiments as SETD8 levels fall. However, importantly, we have provided evidence for a mechanism that involve at least in part active demethylation. Even though there are no confirmed demethylases for H4K20me1, in the conditions we examined, preventing methyltransferase turnover still led to reduced methylation levels (Figure 5).

3.3 MYC as a transcriptional regulator for ribosome biogenesis

MYC regulates ribosomes and protein synthesis in a number of ways including the transcription of ribosomal proteins, cofactors, and the initiation and elongation factors (van Riggelen et al., 2010). MYC also affects translation by promoting mRNA CAP methylation (Cole and Cowling, 2009). Consistent with previous studies that elevated MYC levels resulted in increased binding in actively transcribed MYC target genes and enhance their transcription (Lin et al., 2012), when MYC levels increase in the cell in response to AA depletion, MYC binding accumulates in the promoters of a large group of genes throughout the genome. Even though it remains unclear the exactly mechanism of how the transcription of genes that are enhanced for specific purpose such as protein synthesis is amplified, our observations suggests that larger amount of increase in MYC binding in specific genes may contribute to the transcriptional upregulation. Our data revealed that although elevated MYC can enhance the expression of translation initiation factors, additional changes occurred on chromatin, namely the loss of H4K20me1, as the gene encoding protein components of the ribosomal large and small subunits were upregulated (Figure 13C).

The enhanced expression of all components—translation initiation factors as well as large and small ribosomal proteins—was needed for cells to have a higher capacity for protein synthesis (Figures 14 and 16).

3.4 Metabolic control of translational initiation

It was first observed over forty years ago in Ehrlich ascites tumor and HeLa cells that depletion of one or more amino acids from culture medium reduces overall protein synthesis, a phenotype that is rapidly reversible upon repletion of the nutrients (van Venrooij et al., 1972; Vaughan et al., 1971). It was deduced that the defect occurred mainly at translational initiation, because the rate of synthesis per polyribosome decreased only slightly, and the amount of monomeric ribosomes was increased (van Venrooij et al., 1972). In respond to limiting AAs, mTORC1 inactivation and subsequent activation of autophagosomal-lysosomal pathway would presumably be the mechanism for cells to break down in bulk cytoplasmic proteins and organelles to supply amino acids for translation (Mortimore and Pösö, 1987). However, not all cells and organs are capable of adapting to starvation using autophagy to the same extent (Mizushima et al., 2004), suggesting the possibility of additional mechanism for cells to cope with nutrient shortage. Indeed, acute AA restriction triggers proteasomal protein degradation to rapidly supply amino acids for protein synthesis; and inhibiting proteasome in addition to nutrient starvation resulted in translation impairment (Vabulas and Hartl, 2005).

The role of MYC in various cancers and its role in transcriptional regulation of ribosome biogenesis have been well characterized (van Riggelen et al., 2010). Our data has now uncovered the importance of H4K20me1 for the ability of MYC to further enhance translational capacity in response to AA deprivation. Nevertheless, the parallel functions of MYC and chromatin to coordinate a counterintuitive increase in translational capacity when AAs are limiting could prepare the cell for faster recovery when AAs are replenished. This notion may also have

implications for understanding how MYC drives cancer metabolism and progression, especially in the context of enhancing protein biosynthesis in cancer (Cunningham et al., 2014).

CHAPTER 4

Experimental procedures

4.1 Cell culture

HeLa and IMR90 cells were maintained in DMEM (Cellgro #10-013-CV) supplemented with 10% fetal bovine serum (FBS) (Thermo Fisher HyClone #SV30014.03). HBTEC cells were obtained from Cell Systems and maintained in the recommended medium (Cell Systems #FC-0035). For all experiments with custom media (detailed below), the cells were treated for 16 hrs unless otherwise indicated.

4.2 Media preparation

Custom media were prepared where applicable as indicated in the figures and results. Media containing complete amino acids (AA) were made from DMEM powder (US Biological #D9802) and supplemented with an additional 3.5 g/L D-glucose (for a total of 4.5 g/L), 1 mM sodium pyruvate (Gibco #11360070), 3.7 g/L sodium bicarbonate, and 0.0159 g/L sodium phenol red (US Biological #P4040). Media without AA were made from DMEM without amino acids powder (US Biological #D9800-013) and supplemented with an additional 3.5 g/L D-glucose, 1 mM sodium pyruvate (Gibco #11360070), and 3.7 g/L sodium bicarbonate. pH of media was adjusted to 7.2 by the addition of HCl before being filter sterilized and supplemented with 10% dialyzed FBS (Gibco #26400-044). These +AA and –AA media were used for all experiments comparing the two conditions.

Custom dropout media were made by combining individual components of DMEM from sources as indicated below. A 10X inorganic salt mixture was made according to Earle's balanced salts recipe (Sigma #E7510). D-Glucose was supplemented at 4.5 g/L. Individual amino acids (except glutamine) were made at 100X of the concentrations found in DMEM. Premade solutions of vitamins mixture (Sigma #M6895), sodium pyruvate (Gibco #11360070), and L-glutamine (Gibco #25030081) were used. All dropout media were supplemented with 44 mM sodium bicarbonate. pH was adjusted to 7.2 before being filter sterilized and supplemented with 10%

dialyzed FBS (Gibco #26400-044). Media were conditioned at 37°C and 5% CO_2 for 6 hrs to overnight before adding to cells.

4.3 Acid extraction of histones

Acid extracted histones were prepared as described previously (McBrian et al., 2013a). Specifically, nuclei were collected by lysing 70-80% confluent cells in a 10-cm plate with a hypotonic buffer (10 mM HEPES pH 7.9, 1.5 mM $MgCl_2$, 10 mM KCl, 340 mM sucrose, 10% glycerol, 1 mM DTT, protease inhibitors) and then acid-extracted with H_2SO_4. The proteins were collected with trichloroacetic acid (TCA) precipitation and dissolved in 100 µL water for concentration measurement.

4.4 Whole cell extracts

Cells were pelleted after PBS washing and resuspended in Laemmli buffer (2% SDS, 10% glycerol, 60 mM Tris-HCl pH 6.8). The extract was boiled for 10 min and sheared by passing through a 0.7 mm needle (BD #305156) for 10 times.

4.5 Subcellular fractionation

Chromatin fraction was isolated as described previously (Wysocka et al., 2001). Briefly, nuclei were collected the same way as for acid histone extraction as described above and resuspended in lysis buffer B (3 mM EDTA, 0.2 mM EGTA, 1 mM DTT, protease inhibitors). The nuclear extract was pelleted and resuspended in SDS sample buffer for WB analysis.

4.6 Coomassie gel and Western blotting analyses

Analysis and quantification of protein gels and Western blotting (WB) were performed using the Odyssey Infrared Imaging System (LI-COR Biosciences). Histone protein concentration was initially quantified with the BCA assay (Thermo Scientific #23225) and then normalized between samples by quantifying the four histone bands on gels stained with SimplyBlue (Invitrogen #LC6060, referred as coomassie in figures). After normalizing the concentration, 1 µg of protein was loaded in duplicate gels for WB and a second gel for SimplyBlue staining to ensure equal loading. This step—equal loading of histone based on coomassie staining—is critical for accurate determination of histone modification levels. For WCE and chromatin fraction, samples were initially loaded in equal volumes on a gel stained with SimplyBlue to approximate relative amounts loaded. The loading volume was normalized between samples by quantifying the four histone bands and a region corresponding to the sizes of the proteins to be analyzed in subsequent WB.

WBs were performed on acid-extracted histones for histone modifications, on WCE for SETD8, and on chromatin fraction for MYC. WBs were performed with 15% polyacrylamide gels for histone modifications and with 10% gels for non-histone proteins. The gels were transferred onto Immobilon-FL PVDF membrane (Millipore #IPFL00010). Primary and secondary antibodies and dilutions used are listed in Table 5-2.

4.7 mTORC1 inhibition with rapamycin

The 5 mM Rapamycin (Calbiochem #553211) stock provided by vendor was diluted to a 6 µM working solution with DMSO and added to DMEM at final concentration of 6 or 30 nM [Nick]. Control media were prepared by diluting DMSO into media in the same amount used in the treatment. Cells were treated in Rapamycin or DMSO containing media for 8 hrs.

4.8 Protein synthesis inhibition with cycloheximide

A stock solution of cycloheximide (Sigma #C4859) was diluted to a 1.6 mg/mL working solution with DMSO and added to DMEM at final concentrations ranging from 0.4 to 6.4 µg/mL. Control media were prepared by diluting DMSO into media in the same amount as in the highest amount of treatment. Cells were treated in cycloheximide or DMSO containing media for 16 hrs.

4.9 MYC inhibition with 10058F4

MYC inhibitor 10058F4 was dissolved in DMSO to make a 25 mM stock solution and diluted into +AA or –AA media at a final concentration of 50 or 100 µM. Control media were prepared by diluting DMSO into media at a concentration of 4 µL of DMSO per mL of medium. Cells were cultured for 8 hrs in drug free media followed by 8 additional hrs in media containing the inhibitor or DMSO.

4.10 Flowcytometry analysis

Cells were washed with cold PBS immediately following treatment and dissociated into single cells with trypsin. $1x10^6$ cells were fixed in ethanol and stained with propidium iodide (Invitrogen #P3566) for flow cytometry analysis using the FACSCalibur system (BD Biosciences). DNA content and cell cycle profile were analyzed with the ModFit LT software (Verity Software House).

4.11 Cell viability

Cells were dissociated and stained with Trypan Blue solution (Biorad, #145-0021). Cell viability was assessed using the TC10™ automated cell counter (Biorad, #145-0010).

4.12 Chromatin immunoprecipitation

H4K20me1 and H3K36me3 chromatin immunoprecipitation (ChIP) were performed as described previously (Ferrari et al., 2012). Specifically, after being cultured for 16 hrs in +AA or –AA media, HeLa cells were cross-linked in 1% formaldehyde for 10 min at 37°C and then neutralized with 140 mM glycine for 5 min. Cross-linked cells were scraped from the plates and washed with PBS containing protease inhibitors (Roche #11836145001). $2x10^7$ cells were resuspended in 400 µL of ChIP lysis buffer (1% SDS, 50 mM Tris-HCl pH 8, 20 mM EDTA, protease inhibitors) and incubated for 10 min on ice. Immediately, lysates were sonicated using a Misonix sonicator. Sheared lysates were diluted with dilution buffer (16.7 mM Tris-HCl pH 8, 0.01% SDS, 1.1% Triton X-100, 1.2 mM EDTA, 167 mM NaCl) and pre-cleared with Protein G beads (ThermoFisher #10003D) for 2 hrs before immunoprecipitation (IP). 5% of pre-cleared lysate was saved as input. 100 µL (approximately $5x10^6$ cells) of the lysate was incubated overnight with a given antibody (Table 1). Chromatin-antibody complexes were captured with Protein G beads for 2 hrs. Beads were washed twice each with low salt wash buffer A (140 mM NaCl, 50 mM HEPES pH 7.9, 0.1% SDS, 1% Triton X-100, 0.1% Na-deoxycholate), high salt buffer B (500 mM NaCl, 50 mM HEPES pH 7.9, 0.1% SDS, 1% Triton X-100, 0.1% Na-deoxycholate), LiCl buffer (20 mM Tris-HCl pH 8, 250 mM LiCl, 1 mM EDTA, 0.5% Na-deoxycholate, 0.5% NP-40), and with 1x TE. Protein-DNA complexes were eluted from beads at 65°C once each with 100 µL elution buffer (50 mM Tris-HCl pH 8, 1 mM EDTA) and with 150 µL TE containing 0.67% SDS. Eluates were incubated overnight at 65°C to reverse the cross-links and treated with RNase A and Proteinase K. DNA was subsequently extracted using phenol:chloroform:isoamyl alcohol (Invitrogen #15593031).

RNA Pol II and MYC ChIP experiments were performed using the same procedure as histone methylation ChIP with the following modifications. Lysates for MYC ChIP were sonicated with Bioruptor, and $2x10^7$ cells were used for each IP. Cells for RNA Pol II ChIP were resuspended and sonicated in buffers described in (Lee et al., 2006). Briefly, $6x10^6$ cross-linked cells were

resuspended, incubated for 10 min, and then pelleted once each in 600 µL of lysis buffer 1 (50 mM HEPES-KOH pH 7.5, 140 mM NaCl, 1 mM EDTA, 10% glycerol, 0.5% NP-40, 0.25% Triton X-100, protease inhibitors) at 4°C and in 600 µL of lysis buffer 2 (10 mM Tris-HCl pH 8, 200 mM NaCl, 1 mM EDTA, 0.5 mM EGTA, protease inhibitors) at room temperature. Cells were then sonicated in 200 µL of lysis buffer 3 (10 mM Tris-HCl pH 8, 200 mM NaCl, 1 mM EDTA, 0.5 mM EGTA, 0.1% Na-deoxycholate, 0.5% *N*-lauroylsarcosine, protease inhibitors).

4.13 ChIP sequencing library preparation

DNA obtained from ChIP experiments was quantified using Qubit assays (Invitrogen #Q32854). 2 ng DNA from each ChIP and corresponding input samples were used to prepare libraries using the NuGEN Ovation Ultralow Library System (NuGEN Technologies #0331) or the KAPA LTP kit (KAPA Biosystems #8230) and sequenced with Illumina HiSeq platforms to obtain 50 bp-long reads.

4.14 ChIP-seq data analysis

4.14.1 Alignment of sequencing reads

Reads were aligned to the Human genome (hg19) using Bowtie (Langmead et al., 2009) with parameters that allow up to 2-bp mismatch (-v2) and ensure only unique aligning reads were collected (-m1). For all aligned data files, duplicated reads were removed using Samtools (rmdup) (Li et al., 2009). To estimate ChIP enrichment, IP and corresponding input files were randomly sub-sampled to equalize the number of reads (shuf).

4.14.2 Identification of ChIP enrichment

ChIP enrichment was determined using an algorithm described previously (Ferrari et al., 2012). Briefly, the software allows user to define a window size to tile the genome and a Poisson

distribution p-value cutoff to call a window significant. For all experiments reported in this study, the genome was tiled into 50-bp windows. Significant peaks are defined as those windows with Posisson $p< 10^{-3}$ and the same p value cutoff is met in the two neighboring windows.

4.14.3 Calculation of ChIP enrichment over specific genomic features

The enrichment profiles for significant peaks near TSS or across entire genes were generated using Cis-regulatory Elements Annotation System (CEAS) (Shin et al., 2009). H4K20me1 or H3K36me3 associated genes are those with significant H4K20me1 or H3K36me3 enrichment within the region -1 to +5 kb around the transcription start site (TSS). The enrichments profiles were then used to graph average profiles around TSS and Metagene or to generate heat maps.

4.15 mRNA-seq and chromatin RNA-seq library preparation

For mRNA-seq, total RNA was extracted using the Trizol reagents (Ambion #15596026) and treated with TURBO DNase (Ambion #AM2239). 1 μg of total RNA was used to prepare sequencing library using the Illumina TruSeq RNA sample preparation kit. A mixture of external RNA spike-in controls (Ambion #4456740) was added to total RNA prior to library preparation (Jiang et al., 2011). Libraries were sequenced with Illumina HiSeq platforms to obtain 50 bp-long reads. No spike-in control was added to experiment 2, and 100 bp-long reads were obtained from those two libraries.

For chromatin RNA-seq, subcellular fractionation and sequencing libraries were prepared as described previously (Bhatt et al., 2012) Libraries were sequenced with Illumina HiSeq platforms to obtain 50 bp-long reads.

4.16 RNA-seq data analysis

Reads were mapped to the Human genome (hg19) and to spike-in reference sequences using default parameters of TopHat (Trapnell et al., 2009). SAMMate software (Xu et al., 2011) was

used to determine the transcript RPKM (reads per kilobase of exon per million of reads) for mRNA-seq libraries. The sums of RPKM values from the spike-in controls were used to normalize across samples and to adjust transcripts RPKM.

4.17 Gene ontology analysis

Gene ontology analysis was performed by uploading Genebank accession numbers for gene lists of interest to DAVID Bioinformatics Resources 6.8 (Huang da et al., 2009a, b). Significant GO terms were defined as those terms with a minimal of 10 genes and with a Bonferroni corrected p value< 0.01.

4.18 Motif enrichment analysis

Enriched motifs were identified using the HOMER software (Heinz et al., 2010). The perl script findMotifs.pl was used to find motifs enriched within the region -500 to +750 bp from the TSS of a list of genes. The graphical representations of motif consensus sequences were generated with WebLogo (Crooks et al., 2004).

4.19 siRNA and MYC plasmid transfection

SETD8 (NM_020382) knockdown was performed using a predesigned Dicer-substrate siRNA (DsiRNA) targeting exon 8/UTR of SETD8 (IDT DNA #HSC.RNAI.N020382.12.4). HeLa cells were transfected with 50 nM of DsiRNA using Lipofectamine RNAiMAX (Invitrogen #13778) for 48 to 72 hrs. Control samples were transfected with 50 nM of scrambled negative control DsiRNA (IDT DNA #51-01-19-09). MYC was expressed by a pcDNA3-Myc plasmid (addgene #16011). HeLa cells in 10-cm plates were transfected with 10 μg of DNA using BioT reagent (Bioland Scientific #B01) for 24 to 48 hrs.

4.20 Measuring protein synthesis by pulse labeling

After being cultured with the indicated conditions, cells were washed and incubated in DMEM lacking methionine and cysteine for 15 min at 37°C. The media were replaced with the same DMEM supplemented with 0.1 mCi/mL [^{35}S]-Methionine-Cysteine (PerkinElmer NEG77200) for 30 or 60 min (Bonifacino, 2001). After radioactive labeling, cells were washed twice with cold PBS and collected in 0.5 mL PBS. The labeled cells were resuspended in IP lysis buffer (250 mM NaCl, 50 mM Tris-HCl pH8, 5 mM EDTA, 0.5% NP-40, protease inhibitors), incubated on ice for 30 min, and centrifuged for 5 min at 10000x g. The supernatants were quantified using Qubit protein assay (Invitrogen #Q33212). Equal amount of lysates, as determined by protein concentrations, were precipitated with TCA using BSA as a carrier protein. The precipitated proteins were filtered onto 2.5-cm glass microfiber filter disks (Whatman #1822-025) and washed twice each with ice cold 10% TCA and 100% ethanol. The filters were air dried for 30 min and placed into vials containing scintillation fluid (BD #SX18). [^{35}S]-activity was measured by a liquid scintillation analyzer (PerkinElmer Tri-Carb 2800TR).

4.21 Data availability

All the sequencing data generated in this study have been deposited to the Gene Expression Omnibus database under the accession number GSE100304.

CHAPTER 5

Tables

Table 5-1. Ratios of mRNA RPKM for translational initiation factors and ribosomal proteins

name2	–AA/+AA	siSetd8/Ctrl	MYC/Ctrl	siSetd8+ MYC/Ctrl
EIF1	3.7	1.4	2.9	2.6
EIF4A2	3.2	0.7	3.4	4.5
EIF5	2.7	0.7	2.7	2.0
EIF2S2	2.6	0.7	4.8	4.6
EIF3E	2.5	0.5	3.9	5.9
EIF4B	2.4	0.7	1.9	1.7
EIF3A	2.3	0.4	2.7	1.5
EIF3M	2.1	0.7	3.5	4.4
EIF3J	2.0	0.4	4.7	3.3
EIF1B	1.8	1.0	1.5	1.4
EIF5B	1.8	0.5	4.3	3.4
EIF3L	1.7	0.8	1.2	1.8
EIF3D	1.7	0.9	1.3	1.6
EIF3H	1.7	0.8	3.0	3.0
EIF3F	1.4	1.1	0.9	0.9
EIF2S1	1.4	0.7	1.8	2.1
EIF4G2	1.4	0.4	1.8	1.6
EIF2S3	1.3	0.9	2.8	2.7
EIF6	1.3	1.1	0.9	1.7
EIF2B2	1.2	1.0	1.3	2.1
EIF4A1	1.2	0.8	1.1	1.5
EIF4H	1.0	0.8	1.1	0.8
EIF3B	1.0	0.9	0.8	0.5
EIF2B5	0.9	1.1	0.8	0.9
EIF1AD	0.9	1.3	1.2	1.2
EIF4E2	0.8	1.0	0.7	0.7
EIF4A3	0.7	0.9	0.7	0.9
EIF4G1	0.6	0.9	0.5	0.1
RPL26	4.0	0.6	1.5	1.2
RPL17	2.5	0.9	1.9	3.3
RPL36A	2.4	0.6	0.7	1.6
RPL6	2.4	0.7	1.6	2.1
RPL34	2.3	0.8	1.1	2.9
RPL9	2.2	0.7	0.8	2.4
RPL3	1.9	0.9	1.0	1.8
RPL39	1.9	0.9	0.9	2.8
RPL13A	1.9	1.0	0.9	1.6
RPL10A	1.9	0.9	1.0	2.4
RPL11	1.8	0.8	1.1	2.1
RPL23	1.8	0.8	0.9	2.5
RPL35A	1.8	0.8	0.8	2.1
RPL4	1.8	0.8	1.2	2.4
RPL22	1.7	0.7	1.4	2.4
RPL14	1.7	0.8	1.3	3.1
RPL13	1.7	1.0	0.7	1.0
RPL24	1.7	0.8	0.9	2.3

RPL5	1.6	0.7	0.9	1.6
RPL30	1.6	0.8	0.8	2.1
RPL37A	1.6	0.9	0.8	1.8
RPLP0	1.5	0.8	0.9	1.8
RPL19	1.5	0.9	0.8	2.0
RPL32	1.5	0.9	0.8	2.2
RPL28	1.5	1.1	0.9	1.7
RPL12	1.5	0.6	0.5	0.8
RPL10	1.5	1.1	0.8	1.2
RPL27A	1.5	1.0	0.9	1.6
RPL37	1.4	0.9	0.7	2.3
RPL8	1.4	1.0	0.7	1.2
RPL18	1.4	1.1	0.6	1.2
RPL29	1.4	1.0	0.6	1.4
RPL18A	1.4	1.0	0.6	1.2
RPL27	1.4	0.8	0.8	2.2
RPL7A	1.4	1.0	0.8	1.4
RPL15	1.3	0.9	0.6	1.1
RPL36	1.3	1.0	0.8	1.4
RPLP1	1.3	0.9	0.7	1.4
RPL38	1.3	0.8	0.9	2.1
RPLP2	1.3	1.1	0.6	0.7
RPL35	1.3	0.9	0.7	1.8
RPL23A	1.3	0.9	0.9	2.1
RPL31	0.8	0.7	0.7	4.9
RPS24	2.2	0.7	1.7	3.8
RPS12	2.0	0.6	0.9	2.1
RPS27A	1.9	0.8	1.5	3.5
RPS20	1.9	1.0	0.8	2.0
RPS23	1.9	0.9	1.2	2.8
RPS15A	1.8	0.6	0.3	1.4
RPS6	1.8	0.8	1.4	2.7
RPS25	1.7	0.9	1.1	2.7
RPS18	1.7	0.8	0.9	2.0
RPS13	1.6	0.9	1.0	2.9
RPS7	1.6	0.7	1.1	2.8
RPS8	1.5	0.8	0.9	1.6
RPS21	1.5	1.0	0.8	2.0
RPS5	1.5	1.0	0.8	1.8
RPS9	1.5	1.0	0.7	1.2
RPS4X	1.5	0.8	1.0	2.1
RPS16	1.5	1.1	0.8	2.0
RPS28	1.5	1.1	0.6	1.1
RPS10	1.5	0.1	0.3	0.9
RPS11	1.5	1.0	0.8	1.9
RPS29	1.4	0.8	0.5	1.5
RPS14	1.4	0.9	1.0	2.4
RPS3	1.4	0.9	0.9	1.9
RPS19	1.3	1.0	0.7	1.5
RPS27L	1.3	0.9	0.5	1.2

RPS15	1.2	1.0	0.6	1.3
RPS26	0.5	0.9	0.5	0.8
RPS2	0.2	1.7	11.2	15.5

Table 5-2. Primary and secondary antibodies used in WB and ChIP

Antibodies	Source	Identifier	Dilution
H4K20me1	Abcam	Ab9051	WB: 1/4000 ChIP: 5 µg
H4K20me1 #2 (Extended Data Fig. 1C)	Active Motif	39175	WB: 1/2000
H3K4me2	Abcam	Ab32356	WB: 1/2000
H3K4me3	Abcam	Ab8580	WB: 1 µg/mL
H3K9me1	Active Motif	39681	WB: 1/500
H3K9me2	Abcam	Ab1220	WB: 1/1000
H3K36me1	Abcam	Ab9048	WB: 1/1000
H3K36me3	Abcam	Ab9050	WB: 1 µg/mL
H3K79me2	Grunstein Lab	#532	WB: 1/3000
H4K20me2	Abcam	Ab9052	WB: 1/1000
H4K20me3	Abcam	Ab9053	WB: 1/1000
Phospho-p70 S6 kinase (Thr389)	Cell Signaling	9205	WB: 1/1000
Actin	Santa Cruz	Sc-8432	WB: 1/2000
SETD8 (hPR-SET7)	Millipore	06-1304	WB: 1/500
MYC	Santa Cruz	sc-764	WB: 1/2000 ChIP: 10 µg
RNA Pol II (8WG16)	Covance	MMS-126R	WB: ChIP: 1/50
PhosphoSer2-RNA Pol II CTD	Abcam	Ab5095	WB: ChIP: 5 µg
IRDye® 800CW Goat anti-Rabbit IgG	LI-COR	926-32211	WB: 1/10000
IRDye® 800CW Goat anti-Mouse IgG	LI-COR	926-32210	Wb: 1/10000

CHAPTER 6

References

Abbas, T., Shibata, E., Park, J., Jha, S., Karnani, N., and Dutta, A. (2010). CRL4(Cdt2) regulates cell proliferation and histone gene expression by targeting PR-Set7/Set8 for degradation. Molecular Cell *40*, 9-21.

Albert, M., and Helin, K. (2010). Histone methyltransferases in cancer. Seminars in Cell & Developmental Biology *21*, 209-220.

Bannister, A.J., and Kouzarides, T. (2011). Regulation of chromatin by histone modifications. Cell Res *21*, 381-395.

Bannister, A.J., Zegerman, P., Partridge, J.F., Miska, E.A., Thomas, J.O., Allshire, R.C., and Kouzarides, T. (2001). Selective recognition of methylated lysine 9 on histone H3 by the HP1 chromo domain. Nature *410*, 120-124.

Barski, A., Cuddapah, S., Cui, K., Roh, T.-Y., Schones, D.E., Wang, Z., Wei, G., Chepelev, I., and Zhao, K. (2007). High-Resolution Profiling of Histone Methylations in the Human Genome. Cell *129*, 823-837.

Beck, D.B., Oda, H., Shen, S.S., and Reinberg, D. (2012). PR-Set7 and H4K20me1: at the crossroads of genome integrity, cell cycle, chromosome condensation, and transcription. Genes & Development *26*, 325-337.

Bernstein, B.E., Humphrey, E.L., Erlich, R.L., Schneider, R., Bouman, P., Liu, J.S., Kouzarides, T., and Schreiber, S.L. (2002). Methylation of histone H3 Lys 4 in coding regions of active genes. Proc Natl Acad Sci U S A *99*, 8695-8700.

Bernstein, B.E., Mikkelsen, T.S., Xie, X., Kamal, M., Huebert, D.J., Cuff, J., Fry, B., Meissner, A., Wernig, M., Plath, K.*, et al.* (2006). A bivalent chromatin structure marks key developmental genes in embryonic stem cells. Cell *125*, 315-326.

Bhatt, D.M., Pandya-Jones, A., Tong, A.J., Barozzi, I., Lissner, M.M., Natoli, G., Black, D.L., and Smale, S.T. (2012). Transcript dynamics of proinflammatory genes revealed by sequence analysis of subcellular RNA fractions. Cell *150*, 279-290.

Bonifacino, J.S. (2001). Metabolic labeling with amino acids. Curr Protoc Mol Biol *Chapter 10*, Unit 10 18.

Borun, T.W., Pearson, D., and Paik, W.K. (1972). Studies of histone methylation during the HeLa S-3 cell cycle. J Biol Chem *247*, 4288-4298.

Byvoet, P., Shepherd, G.R., Hardin, J.M., and Noland, B.J. (1972). The distribution and turnover of labeled methyl groups in histone fractions of cultured mammalian cells. Archives of Biochemistry and Biophysics *148*, 558-567.

Chan, C.S., Rastelli, L., and Pirrotta, V. (1994). A Polycomb response element in the Ubx gene that determines an epigenetically inherited state of repression. EMBO J *13*, 2553-2564.

Cole, M.D., and Cowling, V.H. (2009). Specific regulation of mRNA cap methylation by the c-Myc and E2F1 transcription factors. In Oncogene (Nature Publishing Group), pp. 1169-1175.

Congdon, L.M., Houston, S.I., Veerappan, C.S., Spektor, T.M., and Rice, J.C. (2010). PR-Set7-mediated monomethylation of histone H4 lysine 20 at specific genomic regions induces transcriptional repression. In J Cell Biochem, pp. 609-619.

Crooks, G.E., Hon, G., Chandonia, J.M., and Brenner, S.E. (2004). WebLogo: a sequence logo generator. Genome Res *14*, 1188-1190.

Cui, K., Zang, C., Roh, T.-Y., Schones, D.E., Childs, R.W., Peng, W., and Zhao, K. (2009). Chromatin Signatures in Multipotent Human Hematopoietic Stem Cells Indicate the Fate of Bivalent Genes during Differentiation. In Cell stem cell (Nature Publishing Group, a division of Macmillan Publishers Limited. All Rights Reserved.), pp. 80-93.

Cunningham, J.T., Moreno, M.V., Lodi, A., Ronen, S.M., and Ruggero, D. (2014). Protein and nucleotide biosynthesis are coupled by a single rate-limiting enzyme, PRPS2, to drive cancer. Cell *157*, 1088-1103.

Dang, L., White, D.W., Gross, S., Bennett, B.D., Bittinger, M.A., Driggers, E.M., Fantin, V.R., Jang, H.G., Jin, S., Keenan, M.C.*, et al.* (2009). Cancer-associated IDH1 mutations produce 2-hydroxyglutarate. Nature *462*, 739-744.

Feng, Q., Wang, H., Ng, H.H., Erdjument-Bromage, H., Tempst, P., Struhl, K., and Zhang, Y. (2002). Methylation of H3-Lysine 79 Is Mediated by a New Family of HMTases without a SET Domain. Current Biology *12*, 1052-1058.

Ferrari, R., Su, T., Li, B., Bonora, G., Oberai, A., Chan, Y., Sasidharan, R., Berk, A.J., Pellegrini, M., and Kurdistani, S.K. (2012). Reorganization of the host epigenome by a viral oncogene. In Genome Res (Cold Spring Harbor Lab), pp. 1212-1221.

Fritsch, C., Brown, J.L., Kassis, J.A., and Muller, J. (1999). The DNA-binding polycomb group protein pleiohomeotic mediates silencing of a Drosophila homeotic gene. Development *126*, 3905-3913.

Gershey, E.L., Haslett, G.W., Vidali, G., and Allfrey, V.G. (1969). Chemical studies of histone methylation. Evidence for the occurrence of 3-methylhistidine in avian erythrocyte histone fractions. J Biol Chem *244*, 4871-4877.

Goberdhan, D.C., Wilson, C., and Harris, A.L. (2016). Amino Acid Sensing by mTORC1: Intracellular Transporters Mark the Spot. Cell Metab *23*, 580-589.

Greer, E.L., Maures, T.J., Hauswirth, A.G., Green, E.M., Leeman, D.S., Maro, G.S., Han, S., Banko, M.R., Gozani, O., and Brunet, A. (2010). Members of the H3K4 trimethylation complex regulate lifespan in a germline-dependent manner in C. elegans. In Nature (Nature Research), pp. 383-387.

Greer, E.L., and Shi, Y. (2012). Histone methylation: a dynamic mark in health, disease and inheritance. Nature Reviews Genetics *13*, 1-15.

Han, S., and Brunet, A. (2012). Histone methylation makes its mark on longevity. In Trends in Cell Biology, pp. 42-49.

Heinz, S., Benner, C., Spann, N., Bertolino, E., Lin, Y.C., Laslo, P., Cheng, J.X., Murre, C., Singh, H., and Glass, C.K. (2010). Simple combinations of lineage-determining transcription factors prime cis-regulatory elements required for macrophage and B cell identities. Molecular cell *38*, 576-589.

Hempel, K., Lange, H.W., and Birkofer, L. (1968). [Epsilon-N-trimethyllysine, a new amino acid in histones]. Naturwissenschaften *55*, 37.

Huang da, W., Sherman, B.T., and Lempicki, R.A. (2009a). Bioinformatics enrichment tools: paths toward the comprehensive functional analysis of large gene lists. Nucleic Acids Res *37*, 1-13.

Huang da, W., Sherman, B.T., and Lempicki, R.A. (2009b). Systematic and integrative analysis of large gene lists using DAVID bioinformatics resources. Nat Protoc *4*, 44-57.

Huang, H., Sabari, B.R., Garcia, B.A., Allis, C.D., and Zhao, Y. (2014). SnapShot: histone modifications. Cell *159*, 458-458 e451.

Jewell, J.L., Russell, R.C., and Guan, K.-L. (2013). Amino acid signalling upstream of mTOR. In Nat Rev Mol Cell Biol (Nature Publishing Group), pp. 133-139.

Jiang, L., Schlesinger, F., Davis, C.A., Zhang, Y., Li, R., Salit, M., Gingeras, T.R., and Oliver, B. (2011). Synthetic spike-in standards for RNA-seq experiments. In Genome Res (Cold Spring Harbor Lab), pp. 1543-1551.

Katoh, Y., Ikura, T., Hoshikawa, Y., Tashiro, S., Ito, T., Ohta, M., Kera, Y., Noda, T., and Igarashi, K. (2011). Methionine adenosyltransferase II serves as a transcriptional corepressor of Maf oncoprotein. In Molecular Cell, pp. 554-566.

Kera, Y., Katoh, Y., Ohta, M., Matsumoto, M., Takano-Yamamoto, T., and Igarashi, K. (2013). Methionine adenosyltransferase II-dependent histone H3K9 methylation at the COX-2 gene locus. In J Biol Chem, pp. 13592-13601.

Killian, J.K., Kim, S.Y., Miettinen, M., Smith, C., Merino, M., Tsokos, M., Quezado, M., Smith, W.I., Jahromi, M.S., Xekouki, P.*, et al.* (2013). Succinate dehydrogenase mutation underlies global epigenomic divergence in gastrointestinal stromal tumor. Cancer Discov *3*, 648-657.

Kinnaird, A., Zhao, S., Wellen, K.E., and Michelakis, E.D. (2016). Metabolic control of epigenetics in cancer. In Nature reviews Cancer, pp. 694-707.

Kleefstra, T., van Zelst-Stams, W.A., Nillesen, W.M., Cormier-Daire, V., Houge, G., Foulds, N., van Dooren, M., Willemsen, M.H., Pfundt, R., Turner, A.*, et al.* (2009). Further clinical and molecular delineation of the 9q subtelomeric deletion syndrome supports a major contribution of EHMT1 haploinsufficiency to the core phenotype. J Med Genet *46*, 598-606.

Kohlmaier, A., Savarese, F., Lachner, M., Martens, J., Jenuwein, T., and Wutz, A. (2004). A chromosomal memory triggered by Xist regulates histone methylation in X inactivation. In PLoS Biology (Public Library of Science), pp. E171.

Kouzarides, T. (2007). Chromatin Modifications and Their Function. In Cell, pp. 693-705.

Kurotaki, N., Imaizumi, K., Harada, N., Masuno, M., Kondoh, T., Nagai, T., Ohashi, H., Naritomi, K., Tsukahara, M., Makita, Y.*, et al.* (2002). Haploinsufficiency of NSD1 causes Sotos syndrome. Nat Genet *30*, 365-366.

Lachner, M., O'Carroll, D., Rea, S., Mechtler, K., and Jenuwein, T. (2001). Methylation of histone H3 lysine 9 creates a binding site for HP1 proteins. Nature *410*, 116-120.

Langmead, B., Trapnell, C., Pop, M., and Salzberg, S.L. (2009). Ultrafast and memory-efficient alignment of short DNA sequences to the human genome. In Genome Biol (BioMed Central), pp. R25.

Lee, D.H., and Goldberg, A.L. (1996). Selective inhibitors of the proteasome-dependent and vacuolar pathways of protein degradation in Saccharomyces cerevisiae. J Biol Chem *271*, 27280-27284.

Lee, T.I., Johnstone, S.E., and Young, R.A. (2006). Chromatin immunoprecipitation and microarray-based analysis of protein location. In Nature Protocols (Nature Publishing Group), pp. 729-748.

Levine, B., and Yuan, J. (2005). Autophagy in cell death: an innocent convict? J Clin Invest *115*, 2679-2688.

Li, H., Handsaker, B., Wysoker, A., Fennell, T., Ruan, J., Homer, N., Marth, G., Abecasis, G., Durbin, R., and Subgroup, G.P.D.P. (2009). The Sequence Alignment/Map format and SAMtools. In Bioinformatics, pp. 2078-2079.

Lim, U., and Song, M.A. (2012). Dietary and lifestyle factors of DNA methylation. Methods Mol Biol *863*, 359-376.

Lin, C.Y., Lovén, J., Rahl, P.B., Paranal, R.M., Burge, C.B., Bradner, J.E., Lee, T.I., and Young, R.A. (2012). Transcriptional amplification in tumor cells with elevated c-Myc. In Cell, pp. 56-67.

Losman, J.-A., and Kaelin, W.G. (2013). What a difference a hydroxyl makes: mutant IDH, (R)-2-hydroxyglutarate, and cancer. In Genes & Development, pp. 836-852.

Lu, C., and Thompson, C.B. (2012). Metabolic regulation of epigenetics. Cell Metab *16*, 9-17.

Lu, C., Ward, P.S., Kapoor, G.S., Rohle, D., Turcan, S., Abdel-Wahab, O., Edwards, C.R., Khanin, R., Figueroa, M.E., Melnick, A.*, et al.* (2012). IDH mutation impairs histone demethylation and results in a block to cell differentiation. Nature *483*, 474-478.

McBrian, M.A., Behbahan, I.S., Ferrari, R., Su, T., Huang, T.-W., Li, K., Hong, C.S., Christofk, H.R., Vogelauer, M., Seligson, D.B.*, et al.* (2013a). Histone acetylation regulates intracellular pH. Molecular cell *49*, 310-321.

McBrian, M.A., Behbahan, I.S., Ferrari, R., Su, T., Huang, T.W., Li, K., Hong, C.S., Christofk, H.R., Vogelauer, M., Seligson, D.B.*, et al.* (2013b). Histone acetylation regulates intracellular pH. Molecular cell *49*, 310-321.

Mentch, S.J., Mehrmohamadi, M., Huang, L., Liu, X., Gupta, D., Mattocks, D., Gómez Padilla, P., Ables, G., Bamman, M.M., Thalacker-Mercer, A.E.*, et al.* (2015). Histone Methylation Dynamics

and Gene Regulation Occur through the Sensing of One-Carbon Metabolism. In Cell Metab, pp. 861-873.

Mizushima, N., Yamamoto, A., Matsui, M., Yoshimori, T., and Ohsumi, Y. (2004). In vivo analysis of autophagy in response to nutrient starvation using transgenic mice expressing a fluorescent autophagosome marker. In Molecular Biology of the Cell (American Society for Cell Biology), pp. 1101-1111.

Mohan, M., Herz, H.M., Takahashi, Y.H., Lin, C., Lai, K.C., Zhang, Y., Washburn, M.P., Florens, L., and Shilatifard, A. (2010). Linking H3K79 trimethylation to Wnt signaling through a novel Dot1-containing complex (DotCom). Genes Dev *24*, 574-589.

Mortimore, G.E., and Pösö, A.R. (1987). Intracellular protein catabolism and its control during nutrient deprivation and supply. In Annual review of nutrition (Annual Reviews 4139 El Camino Way, P.O. Box 10139, Palo Alto, CA 94303-0139, USA), pp. 539-564.

Murray, K. (1964). The Occurrence of Epsilon-N-Methyl Lysine in Histones. Biochemistry *3*, 10-15.

Nishioka, K., Rice, J.C., Sarma, K., and Erdjument-Bromage, H. (2002). PR-Set7 is a nucleosome-specific methyltransferase that modifies lysine 20 of histone H4 and is associated with silent chromatin. In Molecular Cell, pp. 1201-1213.

Paik, W.K., and Kim, S. (1967). E-N-dimethyllysine in histones. Biochemical and Biophysical Research Communications *27*, 479-483.

Pain, V.M. (1994). Translational control during amino acid starvation. In Biochimie, pp. 718-728.

Park, S.Y., Park, J.W., and Chun, Y.S. (2016). Jumonji histone demethylases as emerging therapeutic targets. Pharmacol Res *105*, 146-151.

Pedersen, M.T., and Helin, K. (2010). Histone demethylases in development and disease. Trends Cell Biol *20*, 662-671.

Poirier, L.A., Wise, C.K., Delongchamp, R.R., and Sinha, R. (2001). Blood determinations of S-adenosylmethionine, S-adenosylhomocysteine, and homocysteine: correlations with diet. Cancer Epidemiol Biomarkers Prev *10*, 649-655.

Rice, J.C., Nishioka, K., Sarma, K., Steward, R., Reinberg, D., and Allis, C.D. (2002). Mitotic-specific methylation of histone H4 Lys 20 follows increased PR-Set7 expression and its

localization to mitotic chromosomes. In Genes & Development (Cold Spring Harbor Lab), pp. 2225-2230.

Rinn, J.L., Kertesz, M., Wang, J.K., Squazzo, S.L., Xu, X., Brugmann, S.A., Goodnough, L.H., Helms, J.A., Farnham, P.J., Segal, E.*, et al.* (2007). Functional demarcation of active and silent chromatin domains in human HOX loci by noncoding RNAs. Cell *129*, 1311-1323.

Rock, K.L., Gramm, C., Rothstein, L., Clark, K., Stein, R., Dick, L., Hwang, D., and Goldberg, A.L. (1994). Inhibitors of the proteasome block the degradation of most cell proteins and the generation of peptides presented on MHC class I molecules. Cell *78*, 761-771.

Ruthenburg, A.J., Li, H., Patel, D.J., and Allis, C.D. (2007). Multivalent engagement of chromatin modifications by linked binding modules. Nat Rev Mol Cell Biol *8*, 983-994.

Santos-Rosa, H., Schneider, R., Bannister, A.J., Sherriff, J., Bernstein, B.E., Emre, N.C., Schreiber, S.L., Mellor, J., and Kouzarides, T. (2002). Active genes are tri-methylated at K4 of histone H3. Nature *419*, 407-411.

Saxton, R.A., and Sabatini, D.M. (2017). mTOR Signaling in Growth, Metabolism, and Disease. In Cell, pp. 960-976.

Schotta, G., Lachner, M., Sarma, K., Ebert, A., Sengupta, R., Reuter, G., Reinberg, D., and Jenuwein, T. (2004). A silencing pathway to induce H3-K9 and H4-K20 trimethylation at constitutive heterochromatin. In Genes & Development (Cold Spring Harbor Lab), pp. 1251-1262.

Schotta, G., Sengupta, R., Kubicek, S., Malin, S., Kauer, M., Callén, E., Celeste, A., Pagani, M., Opravil, S., De La Rosa-Velazquez, I.A.*, et al.* (2008). A chromatin-wide transition to H4K20 monomethylation impairs genome integrity and programmed DNA rearrangements in the mouse. In Genes & Development, pp. 2048-2061.

Schulze, J.M., Jackson, J., Nakanishi, S., Gardner, J.M., Hentrich, T., Haug, J., Johnston, M., Jaspersen, S.L., Kobor, M.S., and Shilatifard, A. (2009). Linking cell cycle to histone modifications: SBF and H2B monoubiquitination machinery and cell-cycle regulation of H3K79 dimethylation. Mol Cell *35*, 626-641.

Sen, P., Shah, P.P., Nativio, R., and Berger, S.L. (2016). Epigenetic Mechanisms of Longevity and Aging. In Cell, pp. 822-839.

Shi, X., Hong, T., Walter, K.L., Ewalt, M., Michishita, E., Hung, T., Carney, D., Pena, P., Lan, F., Kaadige, M.R.*, et al.* (2006). ING2 PHD domain links histone H3 lysine 4 methylation to active gene repression. Nature *442*, 96-99.

Shi, Y., Lan, F., Matson, C., Mulligan, P., Whetstine, J.R., Cole, P.A., Casero, R.A., and Shi, Y. (2004). Histone demethylation mediated by the nuclear amine oxidase homolog LSD1. Cell *119*, 941-953.

Shin, H., Liu, T., Manrai, A.K., and Liu, X.S. (2009). CEAS: cis-regulatory element annotation system. In Bioinformatics, pp. 2605-2606.

Strahl, B.D., and Allis, C.D. (2000). The language of covalent histone modifications. Nature *403*, 41-45.

Tan, M., Luo, H., Lee, S., Jin, F., Yang, J.S., Montellier, E., Buchou, T., Cheng, Z., Rousseaux, S., Rajagopal, N.*, et al.* (2011). Identification of 67 Histone Marks and Histone Lysine Crotonylation as a New Type of Histone Modification. Cell *146*, 1016-1028.

Teperino, R., Schoonjans, K., and Auwerx, J. (2010). Histone methyl transferases and demethylases; can they link metabolism and transcription? In Cell Metab, pp. 321-327.

Tillib, S., Petruk, S., Sedkov, Y., Kuzin, A., Fujioka, M., Goto, T., and Mazo, A. (1999). Trithorax- and Polycomb-group response elements within an Ultrabithorax transcription maintenance unit consist of closely situated but separable sequences. Mol Cell Biol *19*, 5189-5202.

Trapnell, C., Pachter, L., and Salzberg, S.L. (2009). TopHat: discovering splice junctions with RNA-Seq. In Bioinformatics (Oxford University Press), pp. 1105-1111.

Tsai, M.C., Manor, O., Wan, Y., Mosammaparast, N., Wang, J.K., Lan, F., Shi, Y., Segal, E., and Chang, H.Y. (2010). Long noncoding RNA as modular scaffold of histone modification complexes. Science *329*, 689-693.

Tschiersch, B., Hofmann, A., Krauss, V., Dorn, R., Korge, G., and Reuter, G. (1994). The protein encoded by the Drosophila position-effect variegation suppressor gene Su(var)3-9 combines domains of antagonistic regulators of homeotic gene complexes. The EMBO Journal *13*, 3822-3831.

Tsukada, Y.-i., Fang, J., Erdjument-Bromage, H., Warren, M.E., Borchers, C.H., Tempst, P., and Zhang, Y. (2005). Histone demethylation by a family of JmjC domain-containing proteins. Nature *439*, 811-816.

Vabulas, R.M., and Hartl, F.U. (2005). Protein synthesis upon acute nutrient restriction relies on proteasome function. In Science (American Association for the Advancement of Science), pp. 1960-1963.

van Riggelen, J., Yetil, A., and Felsher, D.W. (2010). MYC as a regulator of ribosome biogenesis and protein synthesis. In Nature reviews Cancer, pp. 301-309.

van Venrooij, W.J., Henshaw, E.C., and Hirsch, C.A. (1972). Effects of deprival of glucose or individual amino acids on polyribosome distribution and rate of protein synthesis in cultured mammalian cells. Biochim Biophys Acta *259*, 127-137.

Vaughan, M.H., Pawlowski, P.J., and Forchhammer, J. (1971). Regulation of protein synthesis initiation in HeLa cells deprived of single essential amino acids. In Proceedings of the National Academy of Sciences (National Academy of Sciences), pp. 2057-2061.

Wang, Z., Zang, C., Rosenfeld, J.A., Schones, D.E., Barski, A., Cuddapah, S., Cui, K., Roh, T.-Y., Peng, W., Zhang, M.Q.*, et al.* (2008). Combinatorial patterns of histone acetylations and methylations in the human genome. In Nature Publishing Group (Nature Publishing Group), pp. 897-903.

Ward, P.S., Patel, J., Wise, D.R., Abdel-Wahab, O., Bennett, B.D., Coller, H.A., Cross, J.R., Fantin, V.R., Hedvat, C.V., Perl, A.E.*, et al.* (2010). The common feature of leukemia-associated IDH1 and IDH2 mutations is a neomorphic enzyme activity converting alpha-ketoglutarate to 2-hydroxyglutarate. Cancer Cell *17*, 225-234.

Whetstine, J.R., Nottke, A., Lan, F., Huarte, M., Smolikov, S., Chen, Z., Spooner, E., Li, E., Zhang, G., Colaiacovo, M.*, et al.* (2006). Reversal of histone lysine trimethylation by the JMJD2 family of histone demethylases. Cell *125*, 467-481.

Wu, S., Wang, W., Kong, X., Congdon, L.M., Yokomori, K., Kirschner, M.W., and Rice, J.C. (2010). Dynamic regulation of the PR-Set7 histone methyltransferase is required for normal cell cycle progression. In Genes & Development, pp. 2531-2542.

Wysocka, J., Reilly, P.T., and Herr, W. (2001). Loss of HCF-1-chromatin association precedes temperature-induced growth arrest of tsBN67 cells. In Molecular and Cellular Biology, pp. 3820-3829.

Wysocka, J., Swigut, T., Xiao, H., Milne, T.A., Kwon, S.Y., Landry, J., Kauer, M., Tackett, A.J., Chait, B.T., Badenhorst, P.*, et al.* (2006). A PHD finger of NURF couples histone H3 lysine 4 trimethylation with chromatin remodelling. Nature *442*, 86-90.

Xiao, M., Yang, H., Xu, W., Ma, S., Lin, H., Zhu, H., Liu, L., Liu, Y., Yang, C., Xu, Y.*, et al.* (2012). Inhibition of α-KG-dependent histone and DNA demethylases by fumarate and succinate that are accumulated in mutations of FH and SDH tumor suppressors. In Genes & Development (Cold Spring Harbor Lab), pp. 1326-1338.

Xu, G., Deng, N., Zhao, Z., Judeh, T., Flemington, E., and Zhu, D. (2011). SAMMate: a GUI tool for processing short read alignments in SAM/BAM format. In Source Code Biol Med (BioMed Central), pp. 2.

Yang, Y., Lu, Y., Espejo, A., Wu, J., Xu, W., Liang, S., and Bedford, M.T. (2010). TDRD3 is an effector molecule for arginine-methylated histone marks. Mol Cell *40*, 1016-1023.

Ye, C., Sutter, B.M., Wang, Y., Kuang, Z., and Tu, B.P. (2017). A Metabolic Function for Phospholipid and Histone Methylation. Molecular cell *66*, 180-193 e188.

Yin, X., Giap, C., Lazo, J.S., and Prochownik, E.V. (2003). Low molecular weight inhibitors of Myc-Max interaction and function. Oncogene *22*, 6151-6159.

Young, N.L., DiMaggio, P.A., and Garcia, B.A. (2010). The significance, development and progress of high-throughput combinatorial histone code analysis. Cell Mol Life Sci *67*, 3983-4000.

Zee, B.M., Levin, R.S., DiMaggio, P.A., and Garcia, B.A. (2010). Global turnover of histone post-translational modifications and variants in human cells. In Epigenetics & Chromatin, pp. 22.